STRUCTURAL BEHAVIOR OF COMPOSITE MATERIALS

By Stephen W. Tsai

Prepared under Contract No. NAS 7-215 by
PHILCO CORPORATION
Newport Beach, California

NATIONAL AERONAUTICS AND SPACE ADMINISTRATION

For sale by the Office of Technical Services, Department of Commerce, Washington, D.C. 20230 -- Price $2.00

ABSTRACT

This study is concerned with the analysis of the structural behavior of composite materials. It is shown that composite materials can be designed to produce a wide range of mechanical properties. Thus, a structural designer now has at his disposal an added dimension in optimum design - the materials optimization.

Two types of composite materials are investigated: the unidirectional fiber-reinforced composite and the laminated anisotropic composite. Analytical relations are derived between the composite material coefficients and the geometric and material parameters of the constituents.

Test specimens made of filament-wound materials are used. The experimental results show that the relations derived in this study are more accurate than existing theories, which include the netting analysis. Reliable data on filament-wound materials, which are now available for the first time, can be used for future investigations of the behavior of filament-wound structures.

CONTENTS

CONTENTS (Continued)

ILLUSTRATIONS

NOMENCLATURE

A_{ij} = $[A]$ = A = in-plane stiffness matrix, in lb/in.

A^*_{ij} = Intermediate in-plane matrix, in lb/in.

A'_{ij} = In-plane compliance matrix, in lb/in.

B_{ij} = $[B]$ = B = stiffness coupling matrix, in pounds

B^*_{ij} = Intermediate coupling matrix, in inches

B'_{ij} = Compliance coupling matrix, in 1/lb

B''_{ij} = Transformed B_{ij}

C = Filament contiguity, where $0 \leq C \leq 1$

C_{ij} = Composite anisotropic stiffness matrix, in psi

$\bar{C}_{ij}$ = Composite orthotropic stiffness matrix, in psi

D_{ij} = $[D]$ = D = flexural stiffness matrix, in lb-in.

D^*_{ij} = Intermediate flexural matrix, in lb-in.

D'_{ij} = Flexural compliance matrix, in 1/lb-in.

E_f = Filament Young's modulus, in psi

E_m = Matrix Young's modulus, in psi

E_{11} = Axial stiffness of unidirectional composite, in psi

E_{22} = Transverse stiffness of unidirectional composite, in psi

F = Stiffness ratio = E_{22}/E_{11}

G_f = Filament shear modulus = $E_f/2(1 + \nu_f)$

G_m = Matrix shear modulus = $E_m/2(1 + \nu_m)$

G = Shear modulus of unidirectional composite, in psi

H^*_{ij} = $[H^*]$ = H^* = Intermediate coupling matrix, in inch ($\neq B^*_{ij}$)

H'_{ij} = $[H']$ = H' = Compliance coupling matrix, in 1/lb ($= \tilde{B}'_{ij}$ [transposed B'_{ij}])

h = Plate thickness, in inches

k = Filament misalignment factor, $k \leq 1$

NOMENCLATURE (Continued)

K_f = Filament areal modulus = $E_f/2(1-\nu_f)$

K_m = Matrix areal modulus = $E_m/2(1-\nu_m)$

M_i = Bending or twisting moment, in pounds

m = Cross-ply ratio

N_i = Stress resultant, in lb/in.

n = Total number of layers

P = Internal pressure, in psi

p = Two-dimensional hydrostatic pressure, in psi

R = Percent resin content by weight or radius of pressure vessel

S_{ij} = Composite anisotropic compliance matrix, in psi

γ_f = Filament specific gravity

γ_m = Matrix specific gravity

ϵ_i = Strain component, in in./in.

ϵ_i^o = In-plane strain component, in in./in.

θ = Orientation of unidirectional filaments or lamination angle, in degrees

κ_i = Bending or twisting curvature, in $(\text{inch})^{-1}$

ν_f = Filament Poisson's ratio

ν_m = Matrix Poisson's ratio

ν_{12} = Major Poisson's ratio of unidirectional composite

ν_{21} = Minor Poisson's ratio of unidirectional composite

$= \nu_{12}E_{22}/E_{11}$

σ_i = Stress components, in psi

X = Resin content by volume = $\dfrac{\gamma_f/\gamma_m}{(100/R) + (\gamma_f/\gamma_m) - 1}$

SECTION I

INTRODUCTION

1.1 COMPOSITE MATERIALS

Composite materials consist of two or more constituent materials bonded together so that the gross properties of the composite are superior to those of the constituents; e.g., the desirable properties (high strength, high stiffness, and low weight) are maintained, while the undesirable properties (low ductility) are suppressed. The present investigation is intended to establish some rational basis of compatibility between two constituent materials of a composite from the mechanical standpoint. Process difficulties in combining two vastly different materials, chemically and metallurgically incompatible, will not be considered here.

The mechanical compatibility is important if the composite material is to be used for structural members. The desired gross properties of the composite can be achieved by selecting the proper constituent materials and putting them together in a proper geometrical arrangement. In short, the present investigation of the structural behavior of composite materials is motivated from the standpoint of the design and optimization of composite materials.

1.2 STRUCTURAL BEHAVIOR OF COMPOSITE MATERIALS

The composite material is treated as a heterogeneous anisotropic continuum. Thus, the structural behavior of the composite material is described by the mechanical constitutive equation of the composite. The material coefficients of this equation describe the extent of mechanical response of the composite under the influence of external loads. The present

investigation is concerned with the relations between these coefficients and the material and geometric parameters of the constituent materials. This will be described further in the next section.

1.3 TYPES OF STRUCTURAL COMPOSITES

Structural composites can be classified basically into two classes: multiphase and laminated. These are discussed in the following paragraphs.

a. Multiphase Composites

The multiphase composite consists of two or more constituent phases, although most available composites contain only two phases. Examples of two-phase composites include[1, 2] cement aggregate, tungsten carbide in cobalt, alumina whiskers in metal, silica fiber phenolics, teflon fiber in plastics, and glass-reinforced plastics. As a mathematical approximation, two-phase materials can be represented by a quasi-homogeneous continuum, i.e., locally heterogeneous but grossly homogeneous. Of the two phases, the stronger, or reinforcing phase, can be approximated as spherical or cylindrical inclusions dispersed in the matrix phase. For example, the aggregates can be regarded as spherical inclusions; the whiskers, fibers, and filaments as cylindrical inclusions. When the inclusions are randomly distributed, the composite is grossly isotropic; when they are orderly distributed, the composite is grossly anisotropic. The type of symmetry of a grossly anisotropic composite depends on the packing arrangement of the inclusions, e.g., tetragonal or orthotropic symmetry for square packing and transversely isotropic for hexagonal packing.

b. Laminated Composites

The laminated composite consists of many layers of multiphase or homogeneous materials bonded together. Examples of laminated composites include plywood, sandwich construction, and reinforced plastics. As a mathematical approximation, laminated composites can be represented by an in-plane homogeneous and transversely heterogeneous continuum. The transverse heterogeneity has a step-wise variation in material properties between layers.

1.4 SCOPE OF INVESTIGATION

The present investigation is concerned with the structural behavior of two types of composite materials: unidirectional fiber-reinforced composites and laminated composites consisting of unidirectional composites. These are discussed in the following paragraphs.

a. Unidirectional Fiber-Reinforced Composites

The unidirectional fiber-reinforced composite is treated as a two-phase material, with the axis of the reinforcing fibers or filaments aligned parallel and packed randomly in the plane transverse to the fiber axis.

The governing constitutive equation of this composite is the generalized Hooke's law. The material coefficients of this equation are expressed as functions of the material and geometric parameters of the constituent materials.

b. Laminated Composites Consisting of Unidirectional Composites

The laminated composite is assembled by bonding together unidirectional layers of identical mechanical properties, with adjacent layers orthogonal to each other (cross-ply) or oriented symmetrically with respect to an arbitrary reference axis (angle-ply).

The governing constitutive equation is the relation between the in-plane stress and moment and the in-plane strain and curvature. The material coefficients of this equation are expressed as functions of the properties of the unidirectional composite and lamination parameters.

For the experimental verification of the theoretical predictions discussed above, test specimens in the shapes of beams, plates, and cylindrical shells are made from glass filament-epoxy resin composites.

SECTION 2

UNIDIRECTIONAL COMPOSITES – THEORY

2.1 INTRODUCTION

The unidirectional filament-reinforced composite consists of a large number of parallel fibers or filaments embedded in a matrix. The governing constitutive equation of this composite material is

$$\sigma_i = C_{ij} \epsilon_j \tag{2.1}$$

where σ_i = the stress components; ϵ_j = engineering (not tensorial) strain components; C_{ij} = the composite stiffness matrix; i, j = 1, 2, . . . , 6.

The objective of this investigation is to derive the composite anisotropic moduli as functions of the following material and geometric parameters:

$$C_{ij} = C_{ij} (E_f, \nu_f, \gamma_f, E_m, \nu_m, \gamma_m, R, C, k, \theta) \tag{2.2}$$

where E, ν, γ = the Young's modulus, Poisson's ratio, and specific gravity of the filament and matrix, designated by subscripts f and m, respectively; R = matrix (resin) content by weight; C = contiguity factor; k = filament misalignment factor; and θ = orientation of filament axis. The derivation of Equation (2.2) can be simplified considerably by taking advantage of the transformation property of the composite moduli, i.e., Equation (2.2) can be written as

$$C_{ij} = C_{ij} (\bar{C}_{ij}, \theta) \tag{2.3}$$

where $\bar{C}_{ij}$ = the principal components of the stiffness matrix C_{ij}.

Similar studies have been undertaken in recent years; in these studies, the composite media were assumed to be locally heterogeneous and grossly homogeneous with the following additional specializations:

(1) Local and gross isotropy[3-6]

(2) Local anisotropy and gross isotropy[7]

(3) Local isotropy and gross anisotropy[8-14]

The present problem is concerned with (3). Most of the existing works[8-12] may be considered modifications of Paul's[3] method, since they considered the phases connected in series or in parallel. To apply Paul's method, the actual filaments, shown in Figure 1, must be reshaped mathematically into a square or rectangular cross section. Hashin and Rosen[13] did not reshape the filaments, but, instead, relocated mathematically the filaments so that a hexagonal or nearly hexagonal array was attained. Herrmann and Pister[14] relocated the filaments into a square array.

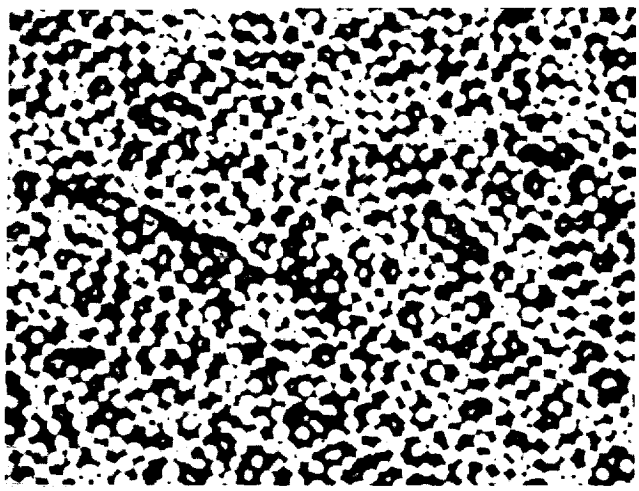

Figure 1. Photomicrograph of Unidirectional Composite

The number of independent moduli increases from two, for the grossly isotropic case, to four, five, or six for the unidirectional composite. The exact number depends on the type of symmetry of the composite, as dictated by the assumed packing arrangement of the fibers in the composite; this is listed as follows:

Symmetry	Number of Independent Moduli	References	Fiber Packing
Orthotropy (Two-Dimensional)	4	6-10	Random
Transverse Isotropy	5	11	Hexagonal or Random
Tetragonal	6	12	Square

For the present investigation, the fiber packing is treated as random, and the symmetry is two-dimensional orthotropy. This viewpoint is realistic, because the unidirectional composite is made in the form of thin plates or layers. Instead of using the components of $\bar{C}_{ij}$, it is more convenient to use the engineering constants E_{11}, E_{22}, ν_{12}, and G, where[15]

$$\bar{C}_{11} = E_{11}/(1 - \nu_{12}\,\nu_{21})$$

$$\bar{C}_{22} = E_{22}/(1 - \nu_{12}\,\nu_{21}) \qquad (2.4)$$

$$\bar{C}_{12} = \nu_{12}\,\bar{C}_{22} = \nu_{21}\,\bar{C}_{11}$$

$$\bar{C}_{66} = G$$

Once the expressions for the four engineering constants in terms of the material and geometric parameters are known, $\bar{C}_{ij}$ and C_{ij} for any value of θ can be computed directly.

2.2 PREDICTION OF E_{11}

The prediction of E_{11}, the composite stiffness parallel to the filaments, is based on the well-known theory that[3, 5, 8, 9, 10, 11, 13]

$$E_{11} = E_f - (E_f - E_m)\, X \tag{2.5}$$

This theory says that the filaments and the matrix are connected in parallel (Paul's upper bound[3]), and each carries a load proportional to its stiffness. This relation must be corrected for filament misalignment factor, k, such that

$$E_{11} = k \left[E_f - (E_f - E_m)\, X\right] \tag{2.6}$$

where

$$X = \text{matrix content by volume} = \frac{\gamma_f / \gamma_m}{(100/R) + (\gamma_f / \gamma_m) - 1} \; ; \; k \leq 1$$

This factor takes into account the fact that the filaments may not be exactly parallel or not perfectly straight. This misalignment is the result of manufacturing processes of the composite material.

2.3 PREDICTION OF E_{22}

The transverse stiffness, E_{22}, of a unidirectional composite can be derived by considering the filaments as parallel cylindrical inclusions. This problem can be regarded as analogous to Hashin's problem on spherical[4] and cylindrical[13] inclusions. But in the case of high filament content (say, R = 20 percent), many filaments become contiguous, i.e., they are in contact rather than isolated by the matrix, as shown in Figure 1. Thus, the assumptions in Reference 13, that (1) each inclusion is completely enclosed by the matrix and (2) the amount of resin enclosing each inclusion is the same as the average matrix content of the entire composite, must be modified. Hence, filament contiguity must be incorporated in the theoretical prediction of E_{22}.

The problem of filament contiguity can be resolved by taking two extreme cases: (1) all filaments are isolated; (2) all filaments are contiguous. The actual packing of the filaments is represented by a linear combination of the two extreme cases. Numerical values of C (for contiguity) can be assigned to the extreme cases, C = 0 for the isolated filaments and C = 1 for the contiguous filaments. The resulting relation of E_{22} is[16, 17, 19]

$$E_{22} = 2\left[1 - \nu_f + (\nu_f - \nu_m)X\right]\left[(1 - C)\frac{K_f(2K_m + G_m) - G_m(K_f - K_m)X}{(2K_m + G_m) + 2(K_f - K_m)X} + C\frac{K_f(2K_m + G_f) + G_f(K_m - K_f)X}{(2K_m + G_f) - 2(K_m - K_f)X}\right] \tag{2.7}$$

where

$$K_f = E_f/2(1 - \nu_f)$$

$$K_m = E_m/2(1 - \nu_m)$$

$$G_f = E_f/2(1 + \nu_f)$$

$$G_m = E_m/2(1 + \nu_m)$$

$$0 \leq C \leq 1$$

The actual value of C is expected to be closer to 0 than to 1 because the latter case replaces the filament in contact by a continuous phase of the filament material. As a comparison, the mathematical models used in References 12-14 correspond to the case of C = 0 (filaments completely isolated).

2.4 PREDICTION OF ν_{12}

The major Poisson's ratio, ν_{12}, can be obtained by considering the isotropic plane of the unidirectional composite to be in a state of plane stress, i.e., $\sigma_x = 0$, where σ_x is the normal stress component along the axis of the

filaments. The amount of lateral contraction, as measured by ϵ_x, is proportional to ν_{12}, so that[18]

$$\nu_{12} = -\frac{E_{11}\ \epsilon_x}{\sigma_y + \sigma_z} = -\frac{E_{11}\ \epsilon_x}{2p} \tag{2.8}$$

where p = two-dimensional hydrostatic pressure.

The effect of filament packing must also be accounted for here as in the prediction of E_{22}. Following the same method as for E_{22}, the resulting relation is[19]

$$\nu_{12} = (1 - C)\frac{K_f\ \nu_f\ (2K_m + G_m)\ (1 - X) + K_m\ \nu_m\ (2K_f + G_m)\ X}{K_f\ (2K_m + G_m) - G_m\ (K_f - K_m)\ X}$$

$$+ C\frac{K_m\ \nu_m\ (2K_f + G_f)\ X \quad + K_f\ \nu_f\ (2K_m + G_f)\ (1 - X)}{K_f\ (2K_m + G_f) + G_f\ (K_m - K_f)\ X} \tag{2.9}$$

Needless to say, the value of C for the major Poisson's ratio and the transverse stiffness must be the same for a given unidirectional composite.

2.5 PREDICTION OF G

The shear modulus, G, of a unidirectional composite is derived by again considering two extreme cases: C = 0, as shown in Reference 13, and C = 1. The resulting relation is

$$G = (1 - C)\ G_m\frac{2G_f - (G_f - G_m)\ X}{2G_m + (G_f - G_m)\ X}$$

$$+ C\ G_f\frac{(G_f + G_m) - (G_f - G_m)\ X}{(G_f + G_m) + (G_f - G_m)\ X} \tag{2.10}$$

Again, the value of C for the gross shear modulus, G, for a given unidirectional composite must be equal to that of the transverse stiffness and the major Poisson's ratio.

2.6 SUMMARY

It is seen that analytical relations have been derived between the independent material coefficients of a unidirectional composite and the material and geometric parameters of the constituent materials. The contribution of each material or geometric parameter can now be ascertained with mathematical precision. For a given structural application it can be easily determined what combination of constituent materials is needed to produce the optimum composite in terms of stress, stiffness or weight.

As a representative glass filament-epoxy resin composite, the following material parameters of the constituents are used in the computation of the composite material moduli:

$$\begin{aligned} E_f &= 10.6 \times 10^6 \text{ psi} \\ \nu_f &= 0.22 \\ \gamma_f &= 2.60 \\ E_m &= 0.5 \times 10^6 \text{ psi} \\ \nu_m &= 0.35 \\ \gamma_m &= 1.15 \end{aligned} \qquad (2.11)$$

The contribution of the filament stiffness E_f to the composite moduli E_{11}, E_{22}, and G can now be illustrated. By increasing the value of E_f to 16.0×10^6 psi, which corresponds to the high-modulus glass, or decreasing E_f to 6.0×10^5 psi while keeping constant all the remaining values of Equation (2.11), the composite moduli are computed. The values used for the filament misalignment factor k is 1.0, and the filament contiguity factor C is 0.2. These values were found to be reasonable for filament-wound materials, as will be seen in the next section. The computed results of the composite moduli are shown in Figure 2. It is clear from the results that the filament stiffness makes the most significant contribution to the axial stiffness E_{11}.

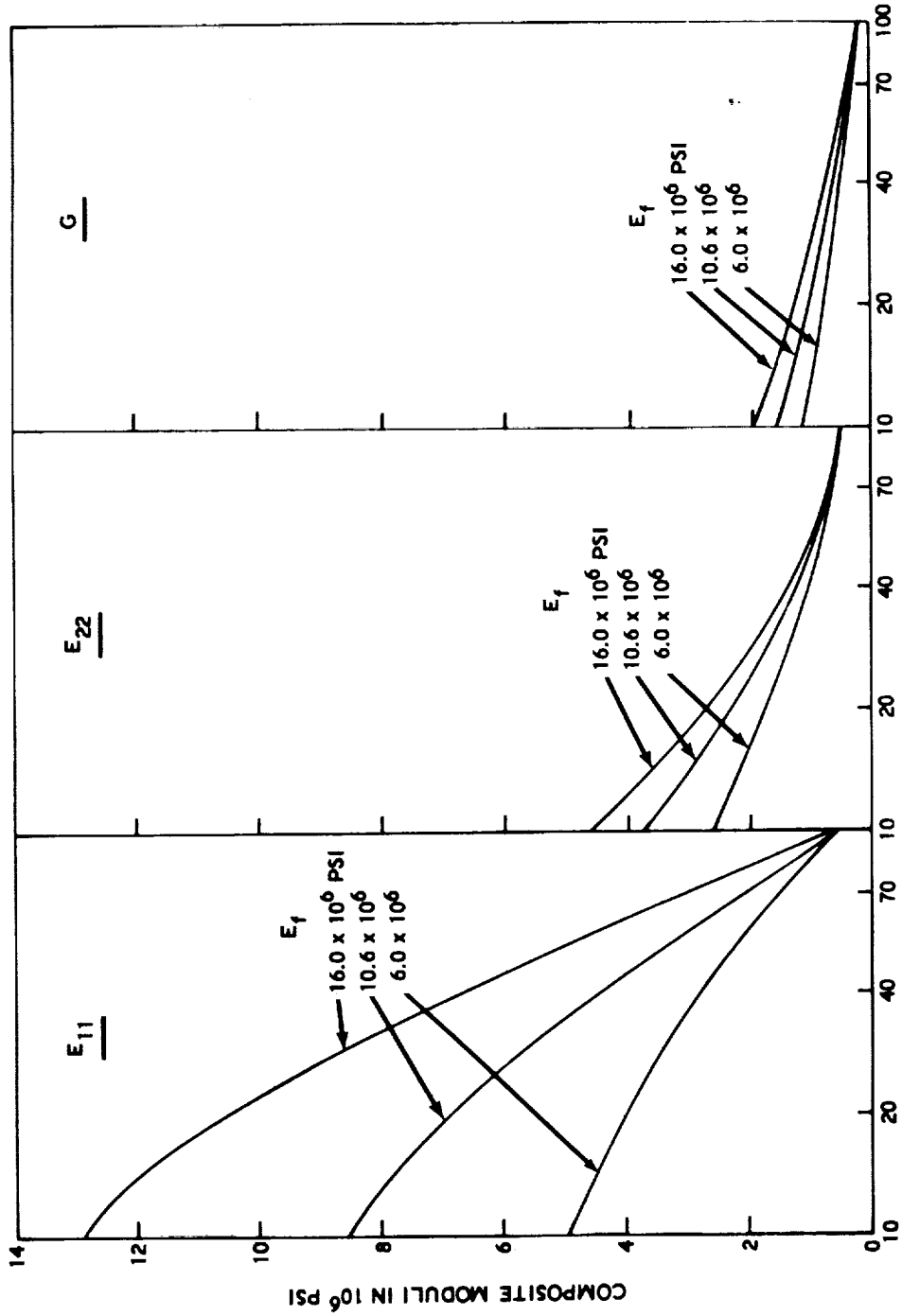

Figure 2. Contribution of E_f to E_{11}, E_{22} and G

Similarly, the contribution of the matrix stiffness E_m to the composite moduli E_{11}, E_{22}, and G can be illustrated by using different values of E_m (1.2 and 0.2×10^6 psi) while keeping all the remaining material parameters in Equation (2.11) constant. The computed moduli are shown in Figure 3, with k = 1.0 and C = 0.2 as before. It is clear from the Figure that the matrix stiffness affects E_{22} and G more than E_{11}.

The effects of Poisson's ratios of the constituent materials on the composite moduli are illustrated in Figure 4 by substituting a number of combinations of Poisson's ratios into the equations for the composite moduli. The axial stiffness is not affected by the Poisson's ratios, because Equation (2.6) does not contain Poisson's ratios. The transverse stiffness and shear modulus do not change significantly by the values of Poisson's ratio. Since most real materials have values of Poisson's ratio between 0.2 and 0.4, the variation of the major Poisson's ratio due to material parameters is not expected to be significant and is, therefore, omitted from the present discussion.

With the composite moduli expressed as analytical functions of the material and geometric parameters, optimization of unidirectional composites can be achieved in a straightforward manner.

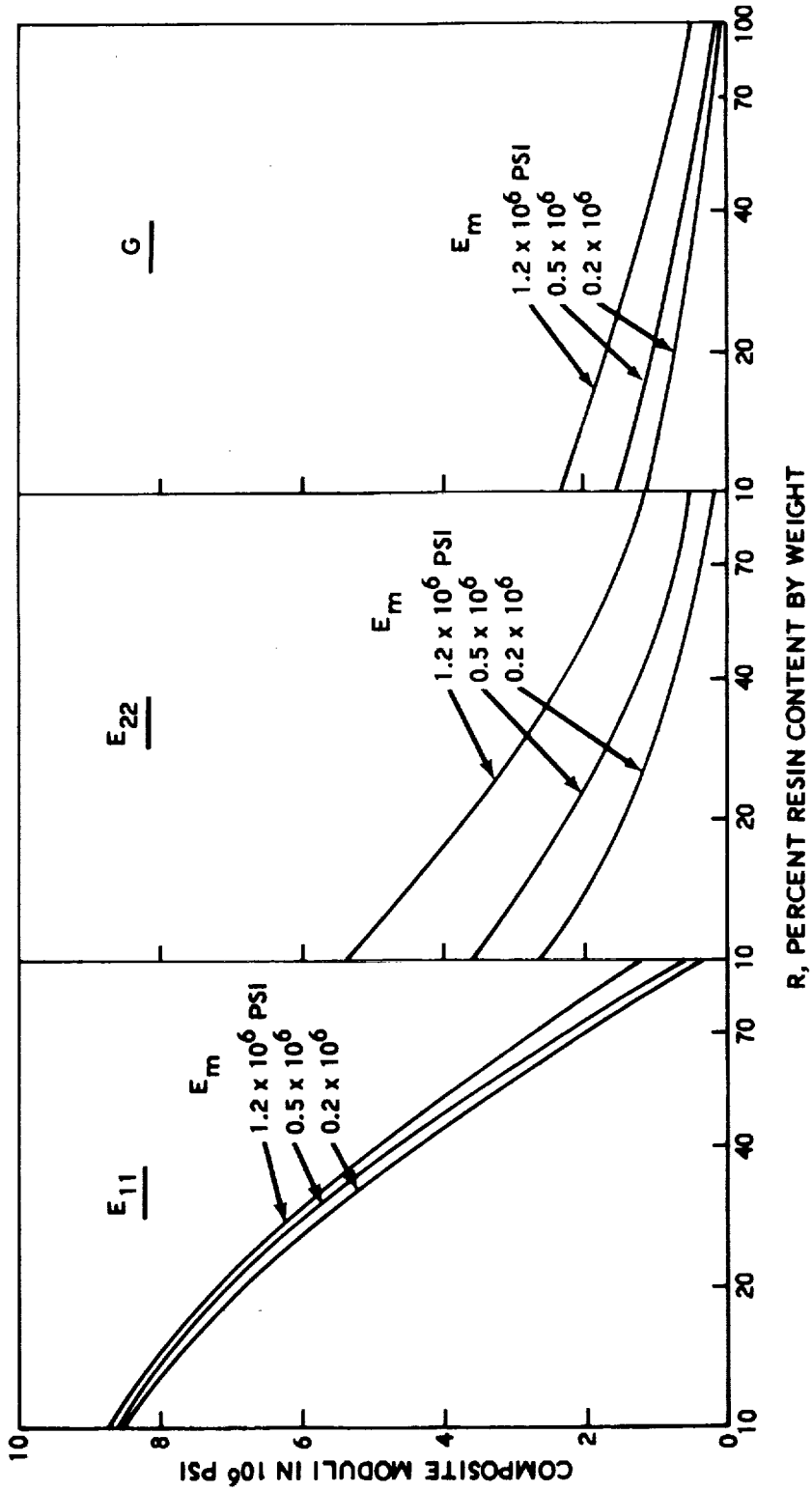

Figure 3. Contribution of E_m to E11, E22 and G

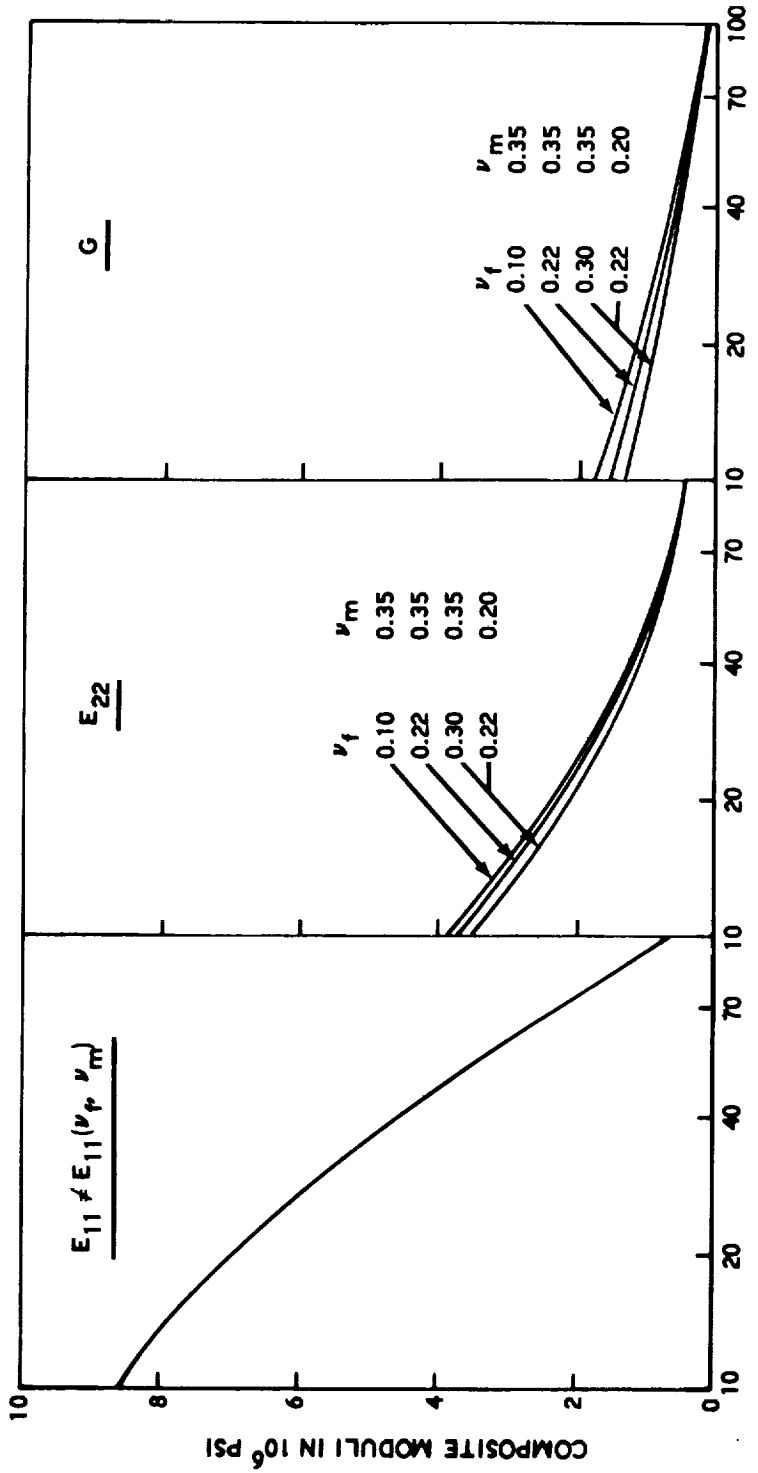

Figure 4. Contribution of ν_m and ν_f to E_{11}, E_{22} and G

SECTION 3

UNIDIRECTIONAL COMPOSITES – EXPERIMENTAL VERIFICATION

3.1 INTRODUCTION

Among all the available investigations on the material coefficients of unidirectional composites, experimental verification of the theoretical predictions is either nonexistent[8, 9, 10, 12, 13, 14] or incomplete.[5, 11] The lack of fundamental data on filament-wound materials has often been cited.[20, 21] Thus, the purpose of this section is twofold: (1) to design critical experiments for the purpose of verifying the theoretical predictions of the preceding section and (2) to provide usable data on a typical unidirectional composite. Filament-wound materials fulfill the requirements best for the following reasons: (1) availability of materials, (2) availability of advanced process technology, and (3) the fact that these materials are in actual use.

Two systems of unidirectional specimens were made. In both cases, unidirectional plies were laid by hand to provide the final thickness. Resin content for each system represents the average of four samples taken from widely spaced locations. The two systems are discussed in the following paragraphs.

a. Scotch-ply

This system consisted of Minnesota Mining and Manufacturing Company Scotch-ply No. 1009-33 W2 38. The curing cycle was: press preheated to 200°F, pressure 40 psi, temperature 300°F for 2 hours, followed by slow cooling. The cured thicknesses ranged between 0.1 to 0.2 inch and the resin contents between 20 to 35 percent.

b. NUF

This system consisted of 11 plies of U.S. Polymeric Company E-787-NUF. The curing cycle was: no preheat, pressure 50 psi, temperature 300°F for 2 hours, followed by slow cooling. The cured thickness was approximately 0.2 inch, and the resin content ranged from 13 to 20 percent.

The experimental determination of the composite anisotropic constants was obtained as follows:

(1) E_{11} and E_{22} were obtained by simple flexural or uniaxial tension tests on 0° and 90° beams (beams cut parallel or transverse to the filaments). Strains were determined from strain rosettes or cross-head motion. The E_{11} and E_{22} obtained from the strain gage readings agreed well with those obtained from simple bending. The implication was that tensile, compressive, and flexural moduli, at least for E_{11} and E_{22}, were essentially the same.

(2) ν_{12} was measured by strain rosettes mounted on 0° beams. The beams were subjected to uniaxial tension or simple bending. Both loading schemes yielded identical data for ν_{12}.

(3) G was measured by imposing a pure twisting moment on a square plate (0° plate). This was accomplished by placing four equal forces at the corners of the square plate. The forces were perpendicular to the plate, with those at the first and third quadrant corners being upward and the second and fourth downward. G was computed from the ratio of the imposed forces and the vertical deflection at the center of the plate in accordance with the elementary theory of plates.

3.2 EXPERIMENTAL RESULTS

In this subsection, the theoretical predictions of the composite moduli are compared with experimental measurements. Glass filament-epoxy resin systems with the following properties were used (same as Equation (2.11)):

$$\begin{aligned} E_f &= 10.6 \times 10^6 \text{ psi} \\ \nu_f &= 0.22 \\ \gamma_f &= 2.60 \\ E_m &= 0.5 \times 10^6 \text{ psi} \\ \nu_m &= 0.35 \\ \gamma_m &= 1.15 \end{aligned} \tag{3.1}$$

Substituting these data into Equation (2.6), E_{11} for k = 1, and 0.9 were computed and are shown in Figure 5, together with experimental points. Practically all points fall between k = 0.9 and 1.0. Since the specimens were laid by hand, filament misalignment was expected to occur. This would result in a k value less than unity.

Using the same data of Equation (3.1), E_{22} was computed from Equation (2.7) for C = 0, 0.2, 0.4, and 1, as shown in Figure 5. It appeared that experimental data agreed with the case of C = 0.2. The E_{22} predicted by the series-connected phases is also shown. Hashin and Rosen's prediction[13] corresponds to the C = 0 case. These predictions yield lower values than those measured. Insofar as netting analysis is concerned, E_{22} is presumed to be equal to zero or E_m; this obviously disagrees with experimental data. The prediction of Herrmann and Pister[14] is also shown; the difference between this prediction and measured data is self-evident. Jacobsen's prediction[12] of E_{22} yields a higher value than E_{11}; this is not reasonable.

The contiguity factor C, though convenient and sound in theory, still needed a more critical verification. For this reason, steel rod-epoxy composites were made with C = 0 (i.e., each rod was completely separated by the resin) and C = 1 (i.e., a steel rod was drilled and subsequently packed with resin). A total of 54 rods or drill holes, arrayed in three rows, made up the composite bar. The rods or drill holes ran transversely to the axis of the bar, as shown in Figure 6.

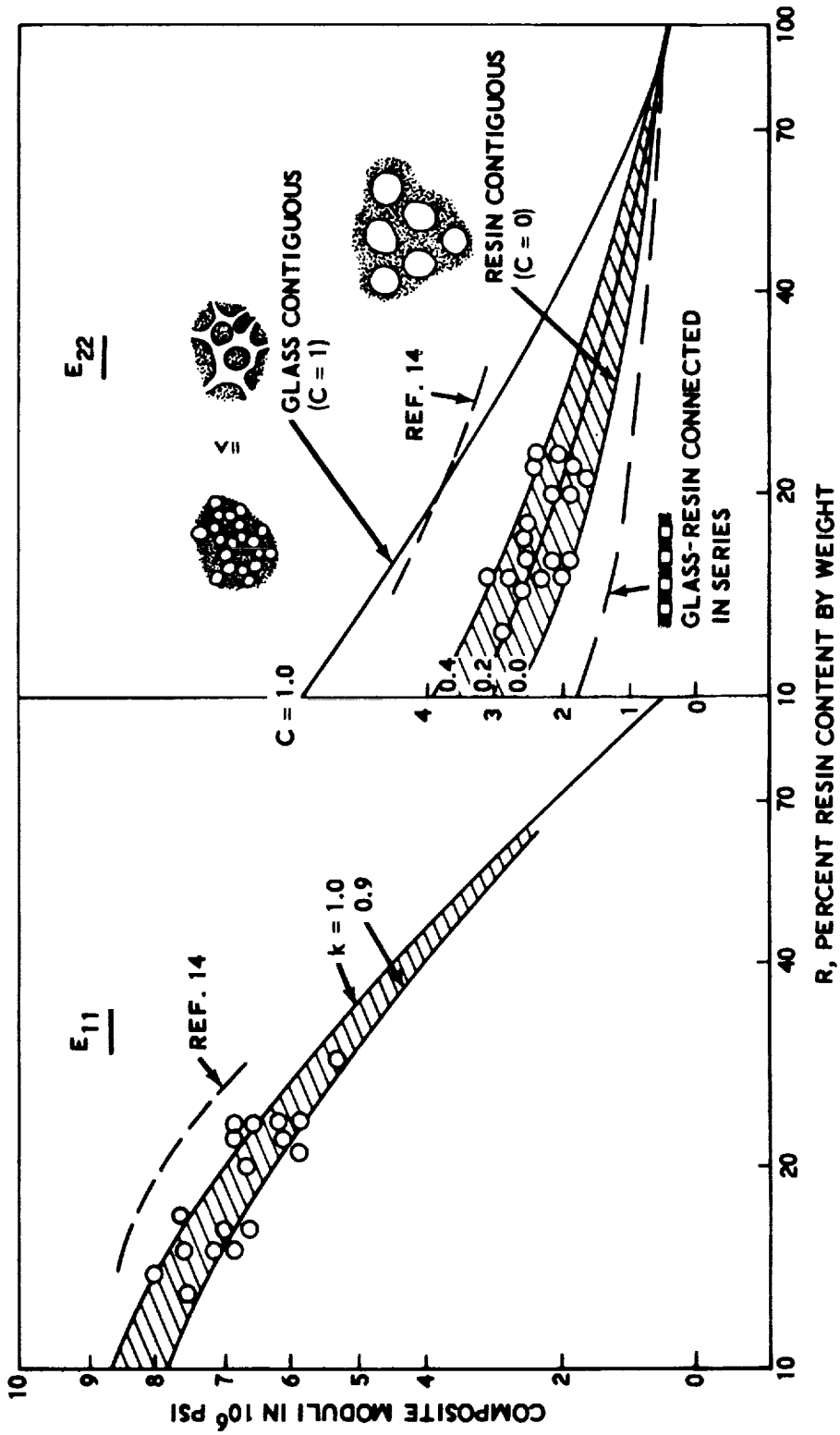

Figure 5. E_{11} and E_{22} Versus R

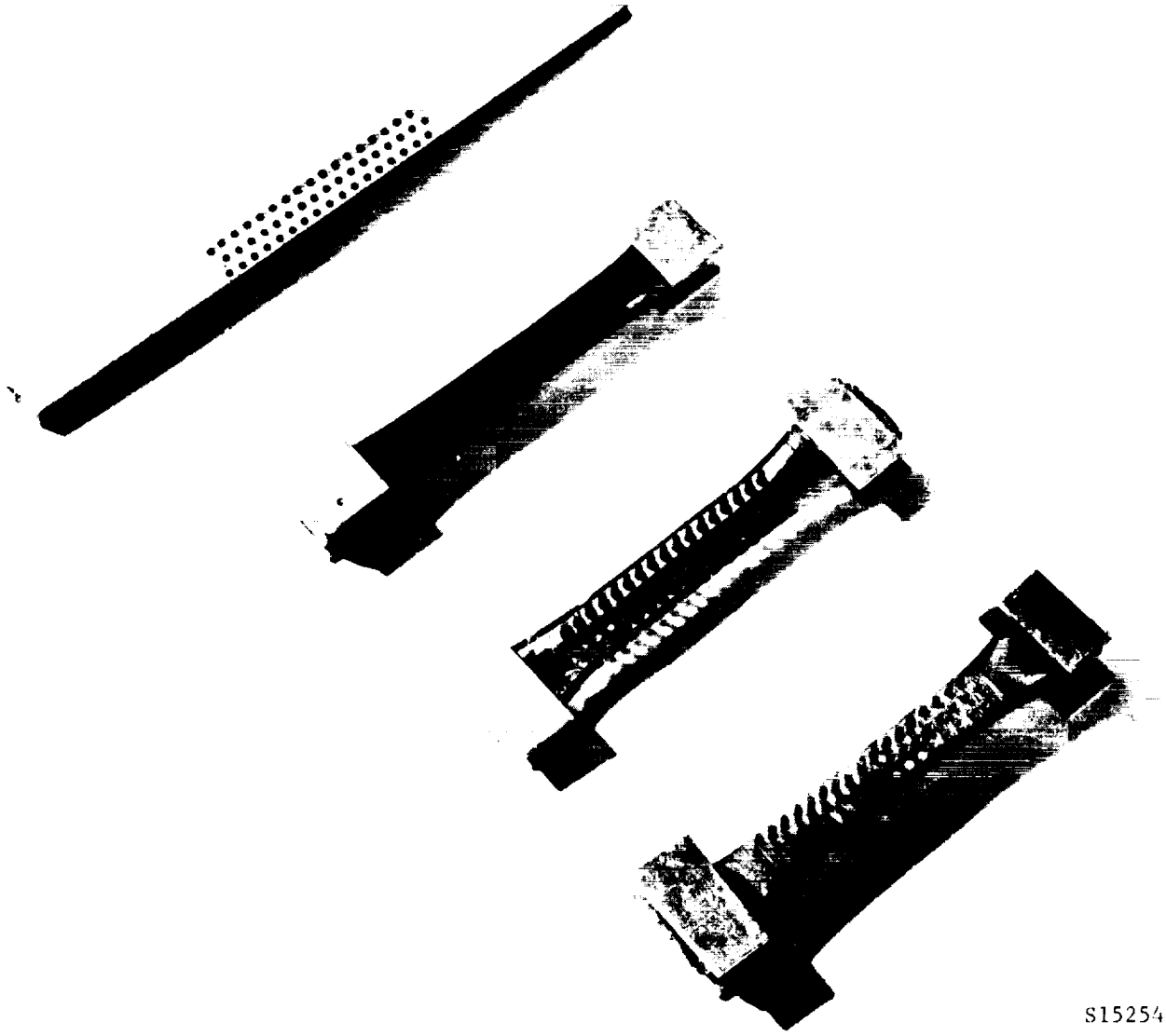

Figure 6. Steel-Epoxy Specimens

Substituting the following data:

$$E_f = 30 \times 10^6 \text{ psi}$$

$$\nu_f = 0.30$$

$$\gamma_f = 7.87$$

$$E_m = \text{as measured (i.e., } 0.45,\ 0.60,\ 0.50 \times 10^6 \text{ psi)} \qquad (3.2)$$

$$\nu_m = 0.35$$

$$\gamma_m = 1.15$$

into Equation (2.7) for C = 0 and 1, the computed results and the measured data are shown in Figure 7. It is seen that the data agreed very well with the C = 0 and 1 cases. These results demonstrated the physical significance of the contiguity factor.

Using the data of Equation (3.1), ν_{12} was computed from Equation (2.9) for C = 0, 0.2, 0.4, and 1. This is shown in Figure 8, together with the measured points. Practically all points fell between C = 0 and 0.4. This is a further verification of the contiguity factor.

Again using the data on Equation (3.1), G was computed from Equation (2.10) for C = 0. 0.2, 0.4, and 1. This is also shown in Figure 8, together with the measured points. Again, all points fell between C = 0 and 0.4. The bounds based on Paul's theory were drawn in dotted lines to illustrate the inaccuracy of this approximate theory when E_f is much greater than E_m. The prediction of G by Herrmann and Pister[14] yielded higher values than those measured, as shown in Figure 8. Hashin and Rosen[13] predicted a much lower value (corresponded to C = 0). In fact, the measured points were higher than the theoretical upper bounds of Reference 13.

3.3 CONCLUSIONS

It is seen that the basic theoretical predictions of the composite moduli of unidirectional filament-wound composites were in agreement with

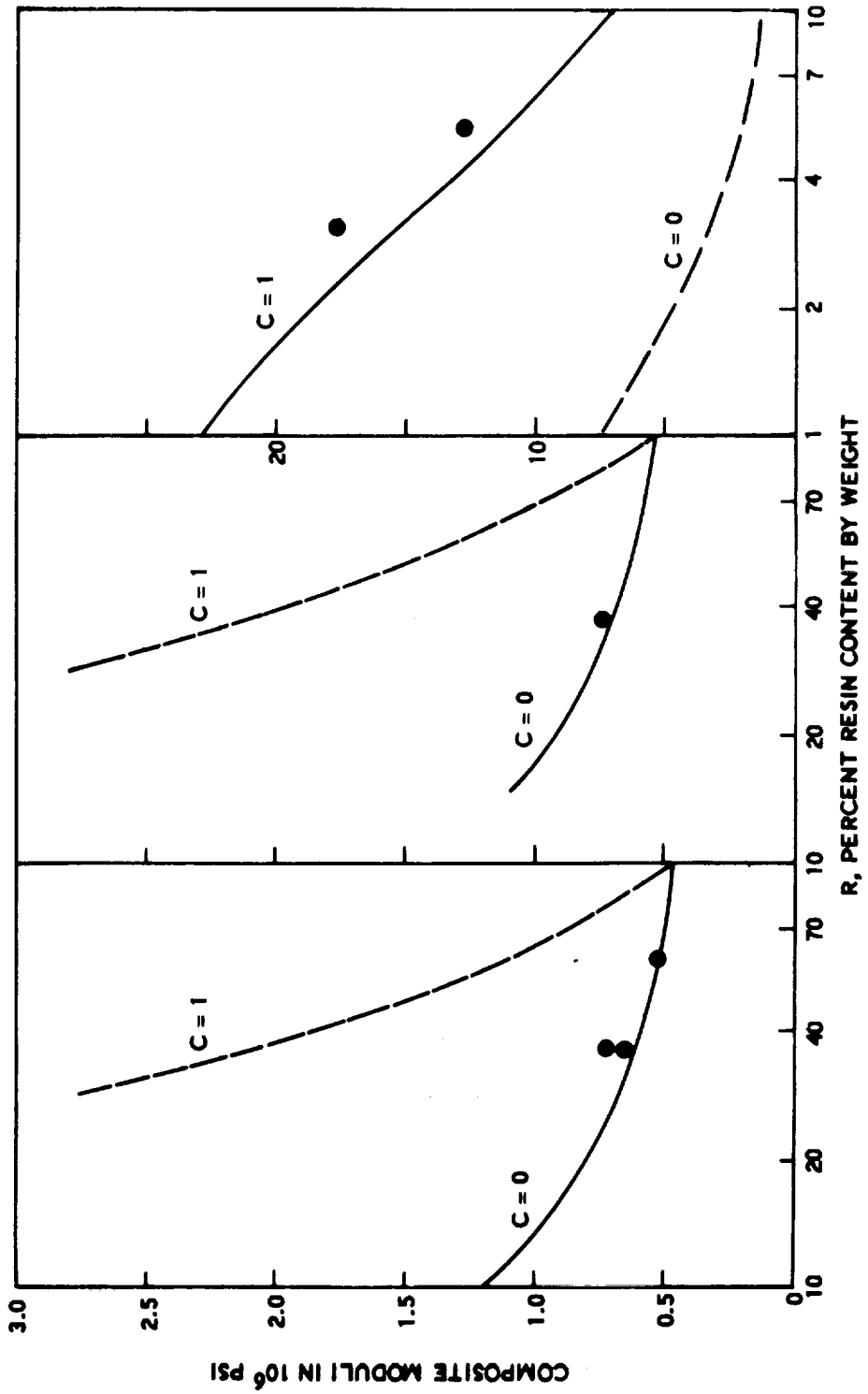

Figure 7. E_{22} of Steel-Epoxy Composites with C = 0 and 1

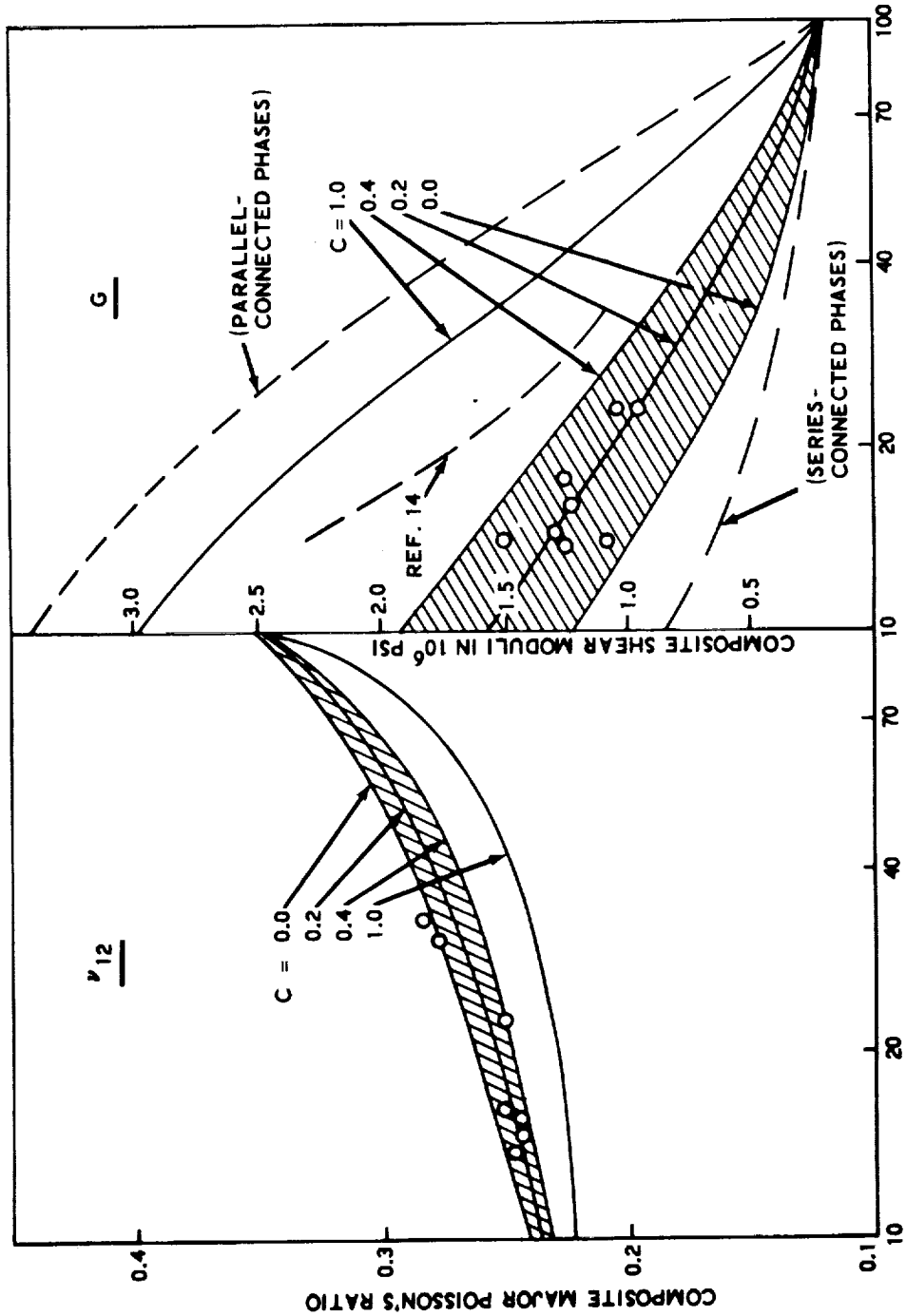

Figure 8. ν_{12} and G Versus R

experimental observations. The contribution of each material parameter to the composite moduli as predicted in the preceding section must be reasonable; thus,

(1) E_f makes a significant contribution to E_{11}.

(2) E_m makes a significant contribution to E_{22} and G.

(3) ν_f and ν_m do not make significant contributions to E_{11}, E_{22}, and G. For this reason, ν_{12} as a function of the material parameters has not been investigated.

Insofar as geometric parameters R, C, and k are concerned, one can conclude:

(1) Matrix content R makes a significant contribution to E_{11}, E_{22}, and G. R is directly related to the weight of the composite.

(2) Contiguity C is probably not a controllable process parameter for the system under investigation. Insofar as stiffness is concerned, a higher value of C increases E_{22}. It is of interest to note that when the E_f and E_m are of the same order of magnitude, the composite moduli for C = 0 and 1 become very close. A fictitious matrix ($E_m = 5.0 \times 10^6$) is combined with a high modulus glass ($E_f = 16.0 \times 10^6$) with a modulus ratio of 3.2. The resultant composite transverse stiffness is shown in Figure 9. The difference between C = 0 and 1 is very small as compared with the same difference in Figure 7. This may be considered as a justification for ignoring contiguity in Hashin's work on tungsten carbide-colbalt composites, for which $E_f/E_m = 3.4$.[4] But for glass-epoxy composites, for which $E_f/E_m = 20$, the effect of contiguity has been shown to be significant.

(3) Filament misalignment k affects E_{11}. This is detrimental in the sense that it decreases its value.

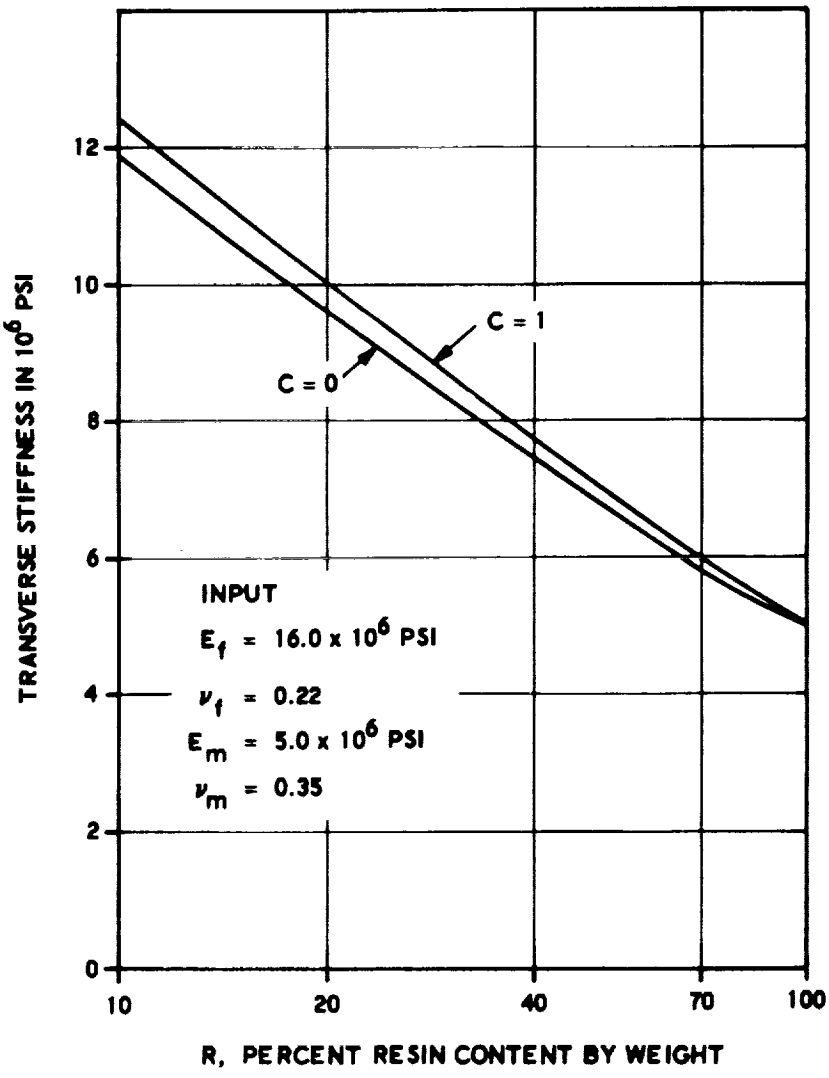

Figure 9. Transverse Stiffness of a Fictitious Composite

It is seen that reliable properties of filament-wound materials are now available. Needless to say, the theory developed in this study is applicable to all fiber-reinforced composites. In succeeding sections, laminated composites consisting of orthotropic unit layers will be investigated.

The mechanical properties of a unidirectional composite can be varied by a wide margin by changing one or several geometric and material parameters. A program of materials optimization in terms of stress, stiffness, and weight can be readily obtained. This provides an added dimension to the designer of structures.

SECTION 4

THEORY OF LAMINATED COMPOSITES

4.1 INTRODUCTION

The laminated composite under present investigation consists of n plies of homogeneous anisotropic sheets. The stress-strain relation of the k^{th} ply is

$$\epsilon_i^{(k)} = S_{ij}^{(k)} \sigma_j^{(k)} \tag{4.1}$$

$$\sigma_i^{(k)} = C_{ij}^{(k)} \epsilon_j^{(k)} \tag{4.2}$$

where $1 \leq k \leq n$; ϵ_i = strain components; σ_i = stress components; S_{ij} = compliance matrix; C_{ij} = stiffness matrix; i, j = 1, 2, 6; and repeated indices represent summation.

In the classical plate theory, the variables used are

$$N_i = \text{stress resultant} = \int_{-h/2}^{h/2} \sigma_i \, dz, \text{ in lb/in.}$$

$$M_i = \text{stress couple} = \int_{-h/2}^{h/2} \sigma_i \, z \, dz, \text{ in lb}$$

ϵ_i^o = in-plane strain, in in./in.

κ_i = bending curvature, in $(\text{in.})^{-1}$

where the total strain $\epsilon_i = \epsilon_i^o + z\,\kappa_i$. Thus the constitutive equation of a laminated anisotropic plate, in matrix form, is

$$\begin{bmatrix} N \\ \\ M \end{bmatrix} = \left[\begin{array}{c|c} A & B \\ \hline B & D \end{array}\right] \begin{bmatrix} \epsilon^o \\ \\ \kappa \end{bmatrix} \tag{4.3}$$

where the composite material matrix is partitioned into four submatrices, so that

$$[A],\ [B],\ [D] = A_{ij},\ B_{ij},\ D_{ij}$$

$$= \int_{-h/2}^{h/2} (1,\ z,\ z^2)\, C_{ij}\, dz, \text{ in lb/in., lb, lb-in.} \tag{4.4}$$

Since each partitioned matrix is symmetric, the composite material matrix is symmetric.

The purpose of the present investigation is to study the nature of A, B, and D matrices as functions of material and lamination parameters. The material parameters refer to the C_{ij} matrix of the unit plies; the lamination parameters refer to the thickness and orientation of each ply and the total number and stacking sequence of all the plies.

4.2 INVERSION OF COMPOSITE MATRIX

It is often more convenient to use the inverted constitutive equations of Equation (4.3). This can be easily accomplished as follows: Equation (4.3) can be written as

$$N = A\,\epsilon^o + B\,\kappa \tag{4.5}$$

$$M = B\,\epsilon^o + D\,\kappa \tag{4.6}$$

From Equation (4.5), $$\epsilon^o = A^{-1} N - A^{-1} B \kappa \tag{4.7}$$

Substituting Equation (4.7) into (4.6) and rearranging,

$$M = B A^{-1} N + (-B A^{-1} B + D) \kappa \tag{4.8}$$

Combining Equations (4.7) and (4.8), in matrix form, gives

$$\begin{bmatrix} \epsilon^o \\ M \end{bmatrix} = \left[\begin{array}{c|c} A^{-1} & -A^{-1} B \\ \hline B A^{-1} & D - B A^{-1} B \end{array}\right] \begin{bmatrix} N \\ \kappa \end{bmatrix} \tag{4.9}$$

$$= \left[\begin{array}{c|c} A^* & B^* \\ \hline H^* & D^* \end{array}\right] \begin{bmatrix} N \\ \kappa \end{bmatrix} \tag{4.10}$$

where the definitions of the star matrices are self-evident. Unlike the composite material matrix of Equation (4.3), the composite star matrix is not symmetric, i.e, $B^* \neq \tilde{H}^*$. This equation is a partial inversion of Equation (4.3). The components of the star matrices are used as the coefficients of the differential equation of equilibrium for laminated plates and shells. Rewriting Equation (4.10),

$$\epsilon^o = A^* N + B^* \kappa \tag{4.11}$$

$$M = H^* N + D^* \kappa \tag{4.12}$$

From Equation (4.12),

$$\kappa = D^{*-1} M - D^{*-1} H^* N \tag{4.13}$$

Substituting Equation (4.13) into (4.12),

$$\epsilon^o = B^* D^{*-1} M + (A^* - B^* D^{*-1} H^*) N \tag{4.14}$$

Combining Equation (4. 13) and (4. 14), in matrix form, gives

$$\begin{bmatrix} \epsilon^{o} \\ \kappa \end{bmatrix} = \left[\begin{array}{c|c} A^{*} - B^{*} D^{*-1} H^{*} & B^{*} D^{*-1} \\ \hline -D^{*-1} H^{*} & D^{*-1} \end{array}\right] \begin{bmatrix} N \\ M \end{bmatrix} \tag{4.15}$$

$$= \left[\begin{array}{c|c} A' & B' \\ \hline H' & D' \end{array}\right] \begin{bmatrix} N \\ M \end{bmatrix} \tag{4.16}$$

where the definitions of the prime matrices are self-evident. Since the composite prime matrix is the inversion of the composite material matrix of Equation (4. 3), it is also symmetric, i. e, $B' = \tilde{H}'$. This equation is the complete inversion of Equation (4. 3). Equation (4. 16) is more convenient to use if the amount of stretching and bending is known for a given problem.

4. 3 THE CONSTITUTIVE EQUATION

Equation (4. 3), or its alternate form as shown in Equation (4. 10) or (4. 16), is the most general constitutive equation for laminated anisotropic plates and shells. Since C_{ij} is a fourth-rank symmetric tensor, A_{ij}, B_{ij}, and D_{ij} must retain the same tensorial properties of C_{ij}, i. e., they are also fourth-rank symmetric tensors. As defined in Equation (4. 4), A_{ij}, B_{ij}, and D_{ij} are obtained by integration along the z axis. This is a scalar operation, which, by definition, does not alter the tensorial property of C_{ij}. Thus, in general, there are 18 independent constants in the present constitutive equation.

If the plate is homogeneous, i. e., C_{ij} is not a function of z,

$$A_{ij} = \frac{12}{h^2} D_{ij}, \qquad B_{ij} = 0 \tag{4.17}$$

The only independent matrix is A; thus, the number of independent constants is at most six.

If the laminated plate consists of isotropic plies only (i.e., it is a generalized sandwich plate),

$$\begin{aligned} C_{11} &= C_{22} \\ C_{66} &= (C_{11} - C_{12})/2 \\ C_{16} &= C_{26} = 0 \end{aligned} \tag{4.18}$$

There are only two independent constants for each unit ply, instead of generally six constants. Thus, for a laminated isotropic plate, A_{ij}, B_{ij}, and D_{ij} each can have at most two independent constants, making a total of six constants. These six constants are, however, different from the six for homogeneous anisotropic plates shown in Equation (4.17).

If the plate is homogeneous and isotropic, the combined conditions of Equation (4.17) and (4.18) reduce the number of independent constants to two.

If the components of C_{ij} are even functions (i.e., C_{ij} is symmetrical with respect to the $z = 0$ plane), B_{ij} is identically zero. The number of independent constants for this type of laminated anisotropic plate is reduced from 18 to 12.

The number of independent constants for a laminated anisotropic composite is affected by the elastic symmetry of the C_{ij} for each unit ply. A general discussion of this subject is too lengthy for the present purpose. Only specific types of laminated plates will be covered, viz., cross-ply and angle-ply composites. It should now be pointed out that in the process of lamination, the elastic symmetry of the original C_{ij} (e.g., orthotropic, angular, cubic, isotropic symmetries), in general, is not carried directly into the laminated plate. The level of symmetry may be increased or decreased, depending on the type of lamination. For a given laminated plate, the elastic symmetries of A_{ij}, B_{ij}, and D_{ij} need not be the same.

SECTION 5

CROSS-PLY COMPOSITES – THEORY

5.1 LAMINATION PARAMETERS

The cross-ply composite consists of n layers of an orthotropic material stacked with alternating orientation of 90° between layers. The principal direction of the odd layers coincide with the x axis, and the even layers with the y axis. All the odd layers have the same thickness. The even layers also have the same thickness, which may be different from that of the odd layers. The lamination parameters of interest are n, the total number of layers, and m, the cross-ply ratio which is defined as the ratio of the total thickness of the odd layers to the total thickness of the even layers.

The purpose of this section is to determine the composite material matrices A, B, and D as functions of the material parameter C_{ij} and lamination parameters m and n.

Assuming each unit layer is homogeneous, the integrations of Equation (4.4) can be replaced by summations, as follows:

$$A_{ij} = \sum_{k=1}^{n} C_{ij}^{(k)} \left(h_{k+1} - h_k\right) \tag{5.1}$$

$$B_{ij} = \frac{1}{2} \sum_{k=1}^{n} C_{ij}^{(k)} \left(h_{k+1}^2 - h_k^2\right) \tag{5.2}$$

$$D_{ij} = \frac{1}{3} \sum_{k=1}^{n} C_{ij}^{(k)} \left(h_{k+1}^3 - h_k^3\right) \tag{5.3}$$

For cross-ply composites, all layers are orthotropic, so that components of the C_{ij} for odd layers are

$$C_{11},\ C_{22},\ C_{12},\ C_{66} \text{ with } C_{16} = C_{26} = 0$$

The components of the C_{ij} for even layers are the same as those for the odd layers, except that C_{11} and C_{22} are interchanged.

5.2 DERIVATION OF A, B, AND D MATRICES

The summations of Equations (5.11), (5.2), and (5.3), can be expressed in closed form for the cross-ply composite. This is accomplished by taking advantage of the properties of series. In a straightforward but laborious manner, the following, where F = the ratio of principal stiffnesses of the unit ply $= C_{22}/C_{11} = E_{22}/E_{11}$, can be derived:

a. For n Odd

$$A_{11} = \frac{1}{1+m}\,(m + F)\,h\,C_{11} \tag{5.4}$$

$$A_{22} = \frac{1}{1+m}\,(1 + m\,F)\,h\,C_{11} = \frac{1 + m\,F}{m + F}\,A_{11} \tag{5.5}$$

$$A_{12} = h\,C_{12} \tag{5.6}$$

$$A_{66} = h\,C_{66} \tag{5.7}$$

$$A_{16} = A_{26} = 0 \tag{5.8}$$

$$B_{ij} = 0 \tag{5.9}$$

$$D_{11} = \left[(F - 1) P + 1\right] \frac{h^3}{12} C_{11} \tag{5.10}$$

$$= \left[(F - 1) P + 1\right] \frac{1 + m}{m + F} \frac{h^2}{12} A_{11} \tag{5.11}$$

$$D_{22} = \left[(1 - F) P + F\right] \frac{h^3}{12} C_{11} \tag{5.12}$$

$$= \left[(1 - F) P + F\right] \frac{1 + m}{m + F} \frac{h^2}{12} A_{11} \tag{5.13}$$

$$D_{12} = \frac{h^3}{12} C_{12} \tag{5.14}$$

$$D_{66} = \frac{h^3}{12} C_{66} \tag{5.15}$$

$$D_{16} = D_{26} = 0 \tag{5.16}$$

where

$$P = \frac{1}{(1 + m)^3} + \frac{m (n - 3) \left[m (n - 1) + 2 (n + 1)\right]}{(n^2 - 1) (1 + m)^3}$$

b. For n Even

Same as the n-odd case, except for the following components:

$$B_{11} = - B_{22} = \frac{m (F - 1)}{n (1 + m)^2} h^2 C_{11} = \frac{m (F - 1)}{n (1 + m) (m + F)} h A_{11} \tag{5.17}$$

$$D_{11} = \left[(F - 1)\, Q + 1\right] \frac{h^3}{12} \quad C_{11} \tag{5.18}$$

$$= \left[(F - 1)\, Q + 1\right] \frac{h^2}{12} \quad \frac{1 + m}{m + F} \quad A_{11} \tag{5.19}$$

$$D_{22} = \left[(1 - F)\, Q + F\right] \frac{h^3}{12} \quad C_{11} \tag{5.20}$$

$$= \left[(1 - F)\, Q + F\right] \frac{h^2}{12} \quad \frac{1 + m}{m + F} \quad A_{11} \tag{5.21}$$

where

$$Q = \frac{1}{1 - m} - \frac{8\, m\, (m - 1)}{n^2\, (1 + m)^3}$$

5.3 DISCUSSIONS OF A, B, AND D MATRICES

Using Equations (5.4) and (5.5), A_{11} and A_{22} are plotted, in dimensionless form, in Figure 10. The remaining components of A are not plotted because either they are identically zero or they remain constant, as shown in Equations (5.6), (5.7), and (5.8). One can conclude that for cross-ply construction:

(1) A_{ij} remains orthotropic.

(2) A_{ij} is independent of n, the total number of plies.

(3) A_{11} and A_{22} are affected drastically by both the stiffness ratio F and the cross-ply ratio m.

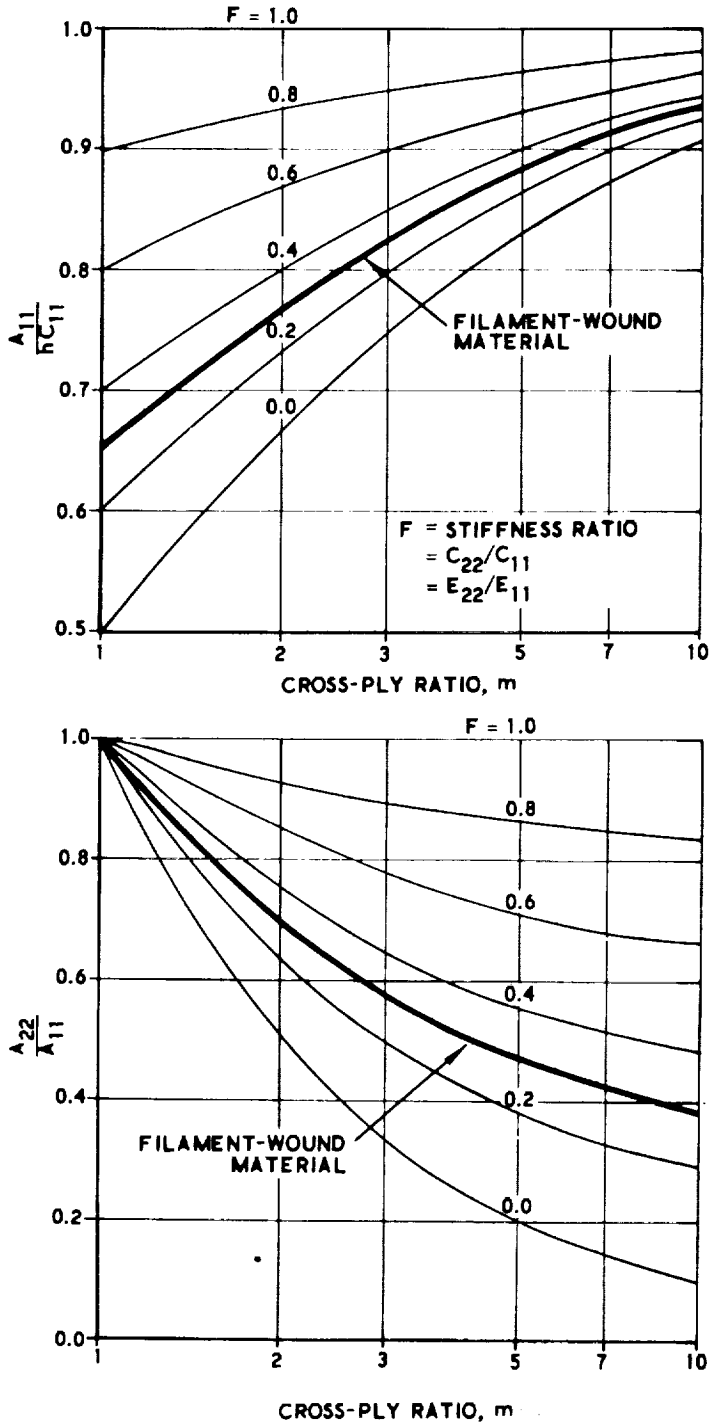

Figure 10. Dimensionless Stiffness Components A_{11} and A_{22}

(4) The average stiffness ratio for filament-wound unidirectional ply is approximately 0.3 for resin contents by weight between 15 and 30 percent. This is also plotted in Figure 10. As a comparison, the stiffness based on netting analysis, which assumes $C_{22} = 0$ or $F = 0$, is also shown. The difference between the two cases, the former case being called the continuum analysis for identification and the latter the netting analysis, is quite substantial. The cross-ply ratio, m, for "balanced design" based on netting analysis is equal to 2.0.

The B_{ij} is identically zero for cross-ply construction except for B_{11}, which is equal to $-B_{22}$, when n is even. Using Equation (5.17), $-B_{11}$ and B_{22} are plotted, in dimensionless form, in Figure 11. The physical significance of B_{11} can be interpreted as a measure of the shifting of the neutral plane. The numerical value in Figure 11 represents the amount of shifting as a fraction of the total plate thickness. The maximum amount of shifting occurs when $n = 2$. The shifting is inversely proportional to n. It becomes small for a large number of plies. It is interesting to observe that this B_{ij} has only one independent component, i.e., B_{11}, with $B_{22} = -B_{11}$ and $B_{12} = B_{66} = B_{16} = B_{26} = 0$. This matrix is more than orthotropic, in the sense that its level of elastic symmetry is higher than the orthotropic case. The transformation property of the B_{ij} is also shown in Figure 11. $B''_{11} = -B''_{22}$ holds for all angles. B''_{12} and B''_{66} remain identically zero. $B''_{16} = B''_{26}$ also holds for all angles. At 45°, $B''_{11} = B''_{22} = 0$; i.e., the shifting of the neutral plane is zero. At this orientation, the cross ply becomes the same as an angle ply, for which the neutral plane does not shift.

The D matrix is much more complicated than the A and B matrices. Since D_{11} and D_{22} depend on both the total number of plies n and stiffness ratio F, only a few combinations of n and F are shown in Figure 12. Again, $F = 0.3$ represents the filament-wound material based on the continuum analysis. First of all, for cross-ply composites D_{ij} is orthotropic. D_{11} and D_{22} approach $h^2 A_{11}/12$ and $h^2 A_{22}/12$, respectively (i.e., the cross-ply composite approaches a homogeneous plate), when: (1) m becomes large, (2) n becomes large, or (3) F approaches 1. For a given cross-ply ratio (say, $m = 2$), the

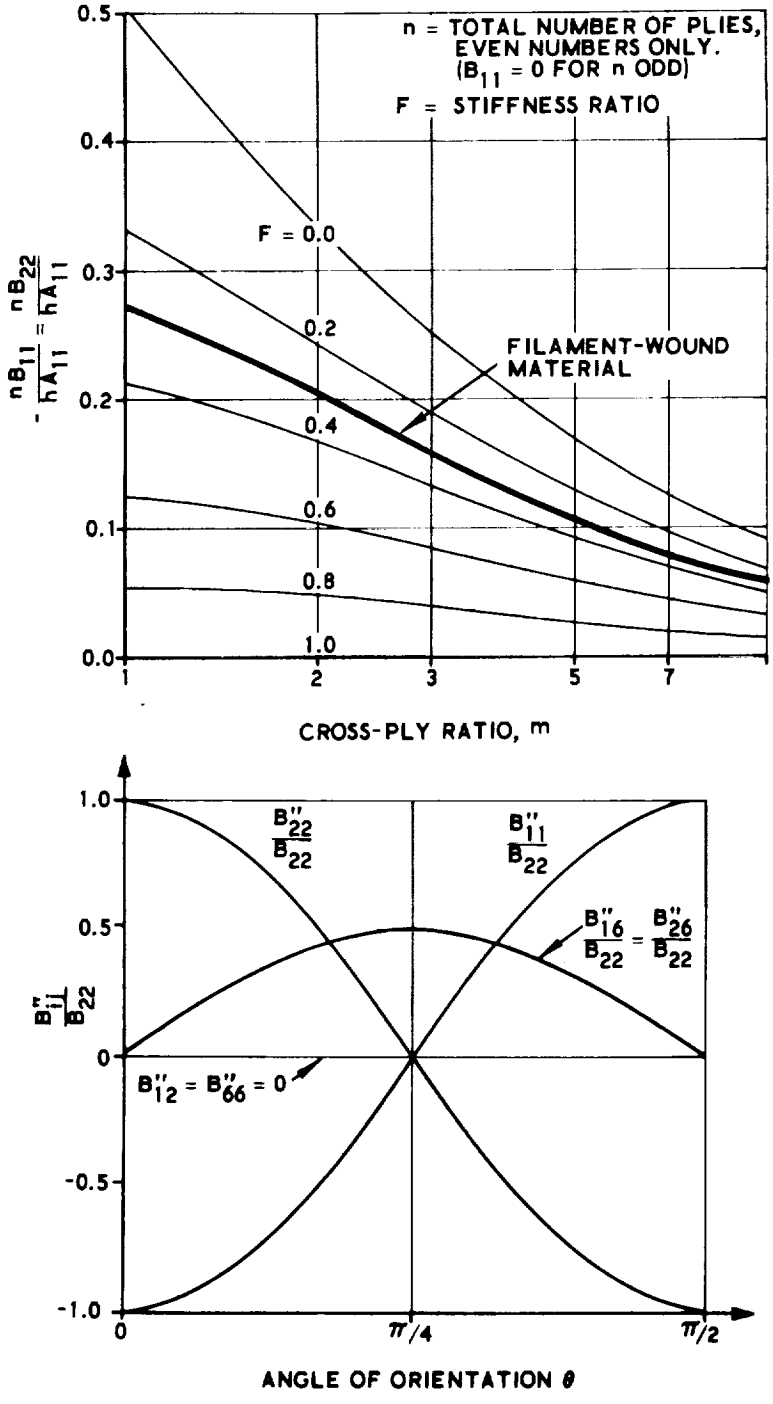

Figure 11. Dimensionless Coupling Term B_{11} and its Transformation Property

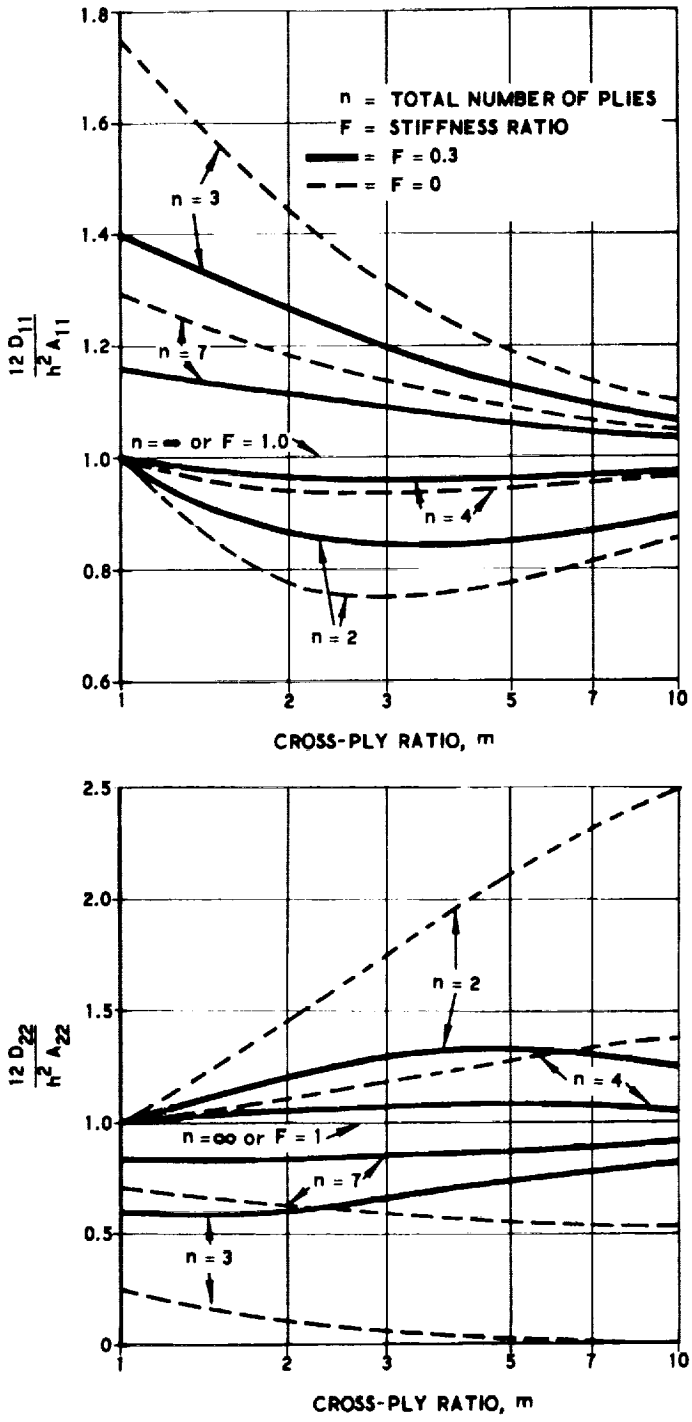

Figure 12. Dimensionless Flexural Rigidities D_{11} and D_{22}

dimensionless flexural rigidities vary significantly, depending on the number of plies, with n = 3 and 2 as the extreme cases for $m \geq 1$. It is seen that an optimum set of material properties can be obtained by using a correct combination of lamination parameters.

Insofar as netting analysis is concerned, the D matrix would be identically zero. This follows directly from the assumptions that the filaments are perfectly flexible and the binding matrix perfectly compliant. Hence, for the D matrix, F = 0 does not correspond to the predictions of the netting analysis.

SECTION 6

CROSS-PLY COMPOSITES – EXPERIMENTAL VERIFICATION

6.1 EXPERIMENTAL PROCEDURE

The purpose of this section is twofold: (1) to establish the validity of the classical theory of laminated plates and (2) to provide usable data for the design of cross-ply composites, which are often used in pressure vessels. Experimental verification is accomplished by comparing the measured material coefficients of laminated composites with the theoretical values derived from the preceding section.

Since all tests were performed by observing the surface strains under the influence of loads or bending moments, it was more direct to compare the theoretical and measured values of the A', B', and D' matrices than the A, B and D matrices. The primed matrices are the coefficients of the constitutive equation in the inverted form, Equation (4.16); the unprimed matrices are the coefficients of the original constitutive Equation, (4.3). Since there is a one-to-one correspondence between the two forms of the constitutive equation, an experimental verification of one of the forms means an equal verification of the other.

All laminated specimens were made of layers of the NUF unidirectional composites. The resin content was approximately 17 percent by weight. The elastic moduli of this unidirectional composite were determined experimentally and found to be in excellent agreement with the theory of unidirectional composites given in Section 2 of this report. The moduli were as given in Equation (6.1) which follows.

$$
\begin{aligned}
E_{11} &= 7.80 \times 10^6 \text{ psi} \\
E_{22} &= 2.60 \times 10^6 \text{ psi} \\
\nu_{12} &= 0.25 \\
G &= 1.25 \times 10^6 \text{ psi}
\end{aligned}
\tag{6.1}
$$

Using these data, the A, B, and D matrices were first computed for various combinations of m (cross-ply ratio) and n (total number of layers). Then the A*, B*, H*, D*, A', B', H', and D' matrices were computed, according to Section 4.

As shown in Section 5, two- and three-layer laminated composites are of special interest, since each represents an extreme case. When the number of layers becomes large, the laminated composite approaches a homogeneous plate very rapidly. Thus, n = 2 and 3 represent the range of variation of the composite properties in a laminated composite. For this reason, all experimental verifications were effectively achieved by testing n = 2 and 3 for various values of m between 1 and 10.

The components of the A', B' and D' matrices were measured by testing 0° and 90° beams. The 0° beams were cut with the axis of the beams running parallel to the axis of the filaments of the odd layers; the 90° beams parallel to the filaments of the even layers. Strain rosettes were mounted on both sides of the beam specimens. The in-plane strain and bending curvature were computed by solving the following simultaneous equations:

$$
\begin{aligned}
\epsilon_i^o + \frac{h}{2} \kappa_i &= \epsilon_i^+ \\
\epsilon_i^o - \frac{h}{2} \kappa_i &= \epsilon_i^-
\end{aligned}
\tag{6.2}
$$

where h = the thickness of the specimen; superscripts plus (+) and minus (-) referred to the strain rosettes mounted on the sides of the specimen; i = 1, 2, and 6.

By applying a uniaxial tension N_1 to a 0° beam, A'_{11}, A'_{12}, B'_{11}, and B'_{12} were measured. By applying a bending moment M_1 to the same beam, D'_{11}, D'_{12}, B'_{11}, and B'_{12} were measured. By repeating the same tests on a 90° beam, A'_{22}, A'_{21}, B'_{22}, B'_{21}, D'_{22}, and D'_{21} were obtained. D_{66} was obtained by imposing a pure twisting test on a 0° square plate. A_{66} was not measured.

6.2 EXPERIMENTAL RESULTS

The experimental results of cross-ply laminated composites of two- and three-layer construction for various cross-ply ratios are shown in Figure 13. The theoretical predictions based on the data given in Equation (6.1) are shown as solid lines. The data for the unidirectional composites, which correspond to $m = \infty$, are shown as $m = 10$. D_{66} remained constant for all values of m. This was confirmed by tests. The results are not shown in Figure 13.

The level of strain was kept below 500 micro-inches per inch. In this range, the load-strain curves were linear and elastic.

6.3 CONCLUSIONS

It is seen that the material coefficients of cross-ply composites can be accurately predicted by using the classical theory of laminated plates. The coupling between the in-plane strain and moment and between curvature and stress resultant is very strong for n even, with $n = 2$ being the strongest. The effect of coupling will give rise to internally induced stresses which are additive to the externally imposed stresses.

Netting analysis, in a very approximate fashion, takes into account the A_{ij} but ignores B_{ij} and D_{ij}. In such an analysis, only the cross-ply ratio m is significant, while the stacking sequence of the unidirectional layers or the total number of layers n is ignored. It is believed that conclusive evidence has been presented here to show that the continuum analysis is more realistic than the netting analysis.

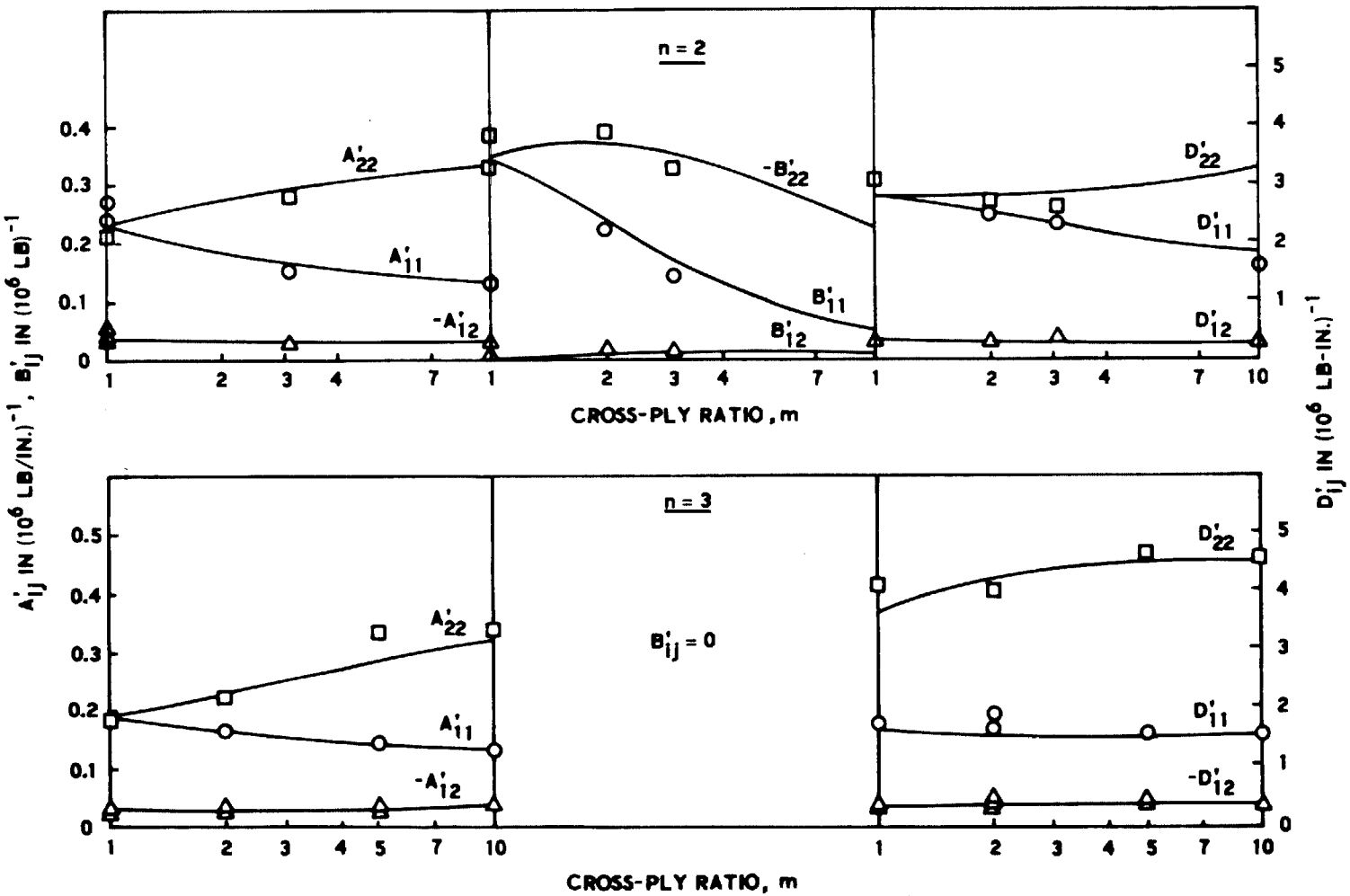

Figure 13. Cross-Ply Composites

SECTION 7

ANGLE-PLY COMPOSITES – THEORY

7.1 LAMINATION PARAMETERS

The angle-ply composite consists of n unit plies of an orthotropic material, with an alternating angle of orientation between layers. The odd plies are orientated with an angle $-\theta$ from the x axis and the even plies $+\theta$. All plies have the same thickness. The lamination parameters for the angle-ply composite are the total number of plies n and the lamination angle θ.

The purpose of this section is to determine the composite material matrices A, B, and D as functions of the material parameter C_{ij} of the unit ply and the lamination parameters n and θ.

7.2 DERIVATION OF A, B, AND D MATRICES

As stated in Section 5.2, the A, B, and D matrices can be obtained by summations shown in Equations (5.1), (5.2) and (5.3). For angle-ply composites, these summations can be further simplified. In fact, A, B, and D can be computed by very simple equations which can be easily derived by expanding the summations and using the conditions of the angle-ply composite (symmetric orientation of unit plies of equal thicknesses). The equations are shown in the

following, where the C_{ij} is the stiffness matrix with $-\theta$ orientation:*

a. For n Odd

$$A_{11},\ A_{22},\ A_{12},\ A_{66} = h\ (C_{11},\ C_{22},\ C_{12},\ C_{66}) \tag{7.1}$$

$$(A_{16},\ A_{26}) = \frac{h}{n}\ (C_{16},\ C_{26}) \tag{7.2}$$

$$B_{ij} = 0 \tag{7.3}$$

$$(D_{11},\ D_{22},\ D_{12},\ D_{66}) = \frac{h^3}{12}\ (C_{11},\ C_{22},\ C_{12},\ C_{66}) \tag{7.4}$$

$$(D_{16},\ D_{26}) = \frac{h^3}{12}\left(\frac{3\,n^2 - 2}{n^3}\right)(C_{16},\ C_{26}) \tag{7.5}$$

b. For n Even

Same as the n odd case, except for the following components:

$$A_{16} = A_{26} = 0 \tag{7.6}$$

$$(B_{16},\ B_{26}) = -\frac{h^2}{n}\ (C_{16},\ C_{26}) \tag{7.7}$$

$$D_{16} = D_{26} = 0 \tag{7.8}$$

---

*The C_{ij} for $+\theta$ orientation is equal to that of the $-\theta$ orientation, except that the sign for C_{16} and C_{26} is changed.

7.3 DISCUSSIONS OF A, B, AND D MATRICES

The absolute values of A_{11} for a representative filament-wound angle-ply composite is plotted against the lamination angle θ in Figure 14. The other components of A_{ij} are also shown in Figure 13 in dimensionless form. A_{11}, A_{22}, A_{12}, and A_{66} are independent of the number of plies, n. A_{16} and A_{26}, however, are dependent on n; when n is even, they are zero; when n is odd, A_{16} and A_{26} are inversely proportional to n. Thus, the maximum absolute values for A_{16} and A_{26} occur when n = 3. It is interesting to note that, for n even, A_{ij} is orthotropic; for n odd, it is not orthotropic, because the plane of elastic symmetry is destroyed. For the latter case, the number of independent constants is six. This is a truly anisotropic system, corresponding to the triclinic case for three-dimensional bodies. According to netting analysis, a lamination angle of $53\text{-}3/4^{\circ}$ is the optimum angle for internally pressurized vessels. According to continuum analysis, there is no reason to restrict the use of the lamination angle to one specific value.

The B matrix for angle-ply composites is identically zero for n odd, but a function of n for n even. The dimensionless B_{16} is plotted in Figure 15. The effect of this ratio can be seen, as follows.

For uniaxial extension, the only non-zero component on the right-hand side of Equation (4.3) is ϵ_1°. Expanding Equation (4.3),

$$
\begin{aligned}
N_1 &= A_{11}\ \epsilon_1^{\circ} \\
N_2 &= A_{12}\ \epsilon_1^{\circ} \\
N_6 &= A_{16}\ \epsilon_1^{\circ} = 0 \\
M_1 &= B_{11}\ \epsilon_1^{\circ} = 0 \\
M_2 &= B_{12}\ \epsilon_1^{\circ} = 0 \\
M_6 &= B_{16}\ \epsilon_1^{\circ}
\end{aligned}
\qquad (7.9)
$$

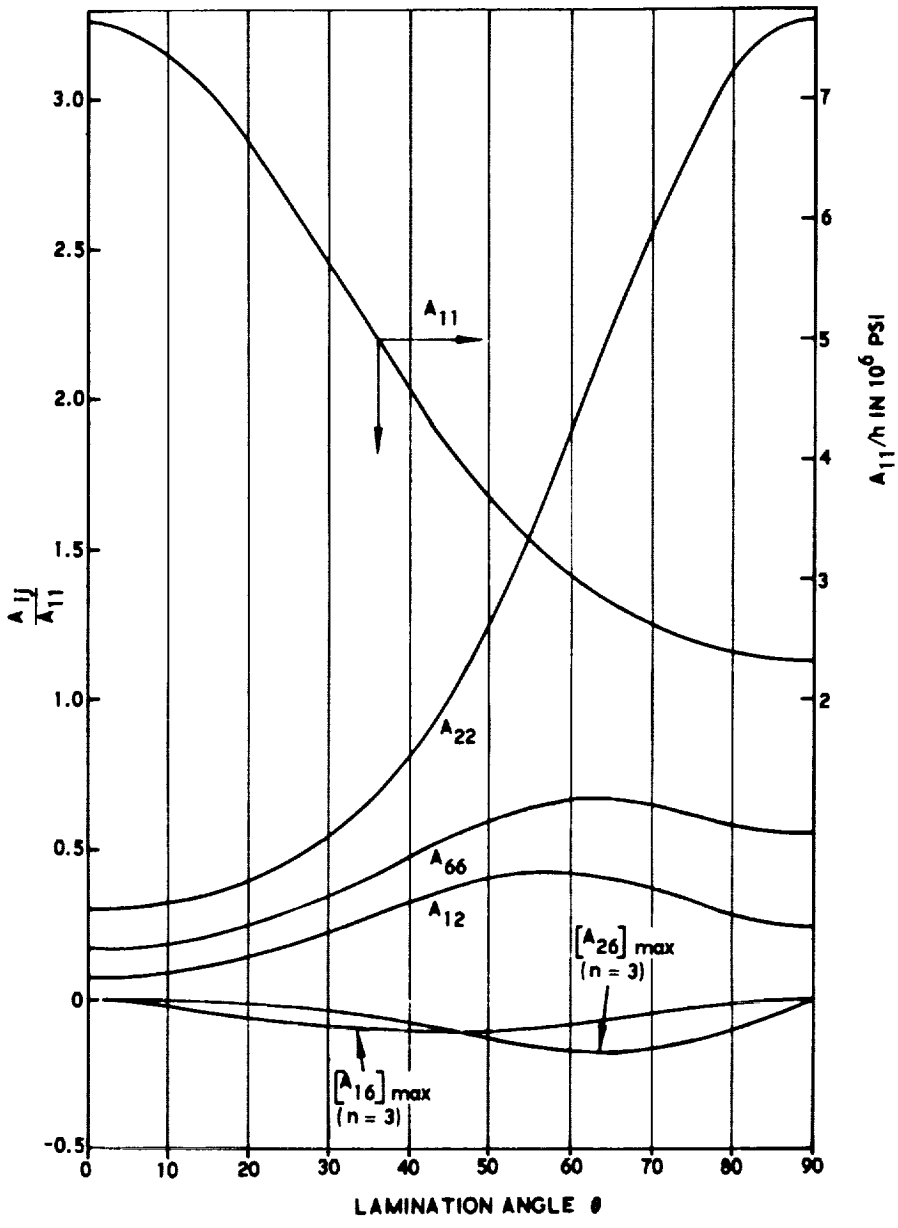

Figure 14. A_{11} and Dimensionless A_{ij} for Representative Filament-Wound Angle-Ply

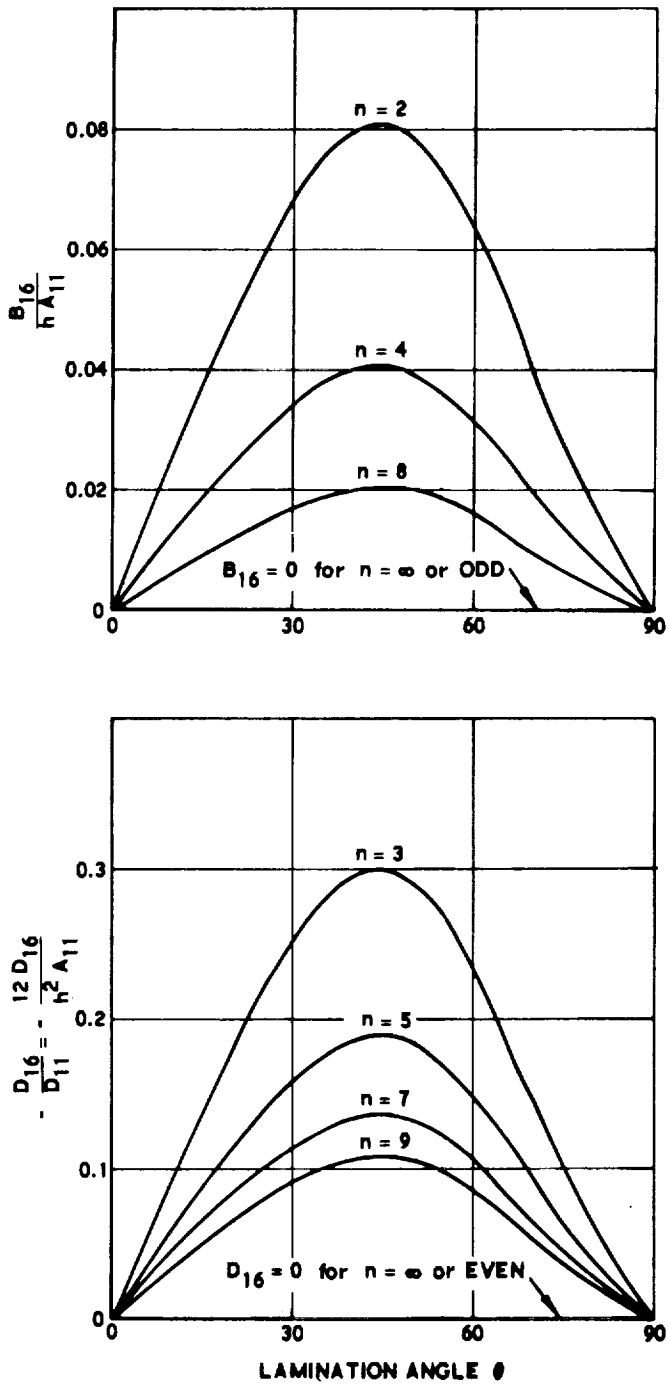

Figure 15. Dimensionless B_{16} and D_{16} for Representative Filament-Wound Angle-Ply

Thus

$$\frac{B_{16}}{h A_{11}} = \frac{M_6}{h N_1} \tag{7.10}$$

This ratio signifies the ratio of the internally induced twisting moment to the in-plane stress resultant. From this ratio can be computed the ratio of the shear stress over the normal stress for the case of uniaxial extension. Similarly, it can be shown that

$$\frac{B_{26}}{h A_{22}} = \frac{M_6}{h N_2} \tag{7.11}$$

This latter ratio has the same numerical value as Equation (7.10), except that the complement of the lamination angle is used for the abscissa.

The case of cross coupling caused by the nonvanishing B_{16} and B_{26} was discussed by Reissner and Stavsky[22] for a two-layer angle ply. From Figure 15 it is clear that this coupling for a representative filament-wound composite is relatively weak. The coupling effect weakens very rapidly as n increases or θ deviates from 45°.

The D matrix for n even remains orthotropic. For n odd, D deviates markedly from orthotropic symmetry; as can be seen from Figure 15 the dimensionless D_{16} is 0.30 for n = 3. This means that for simple bending, the induced twisting moment is 30 percent of the imposed bending moment. This is a very strong coupling and it does not decrease rapidly as n increases. The perturbation technique of Dong and Dong[23] for solving problems of anisotropic plates and shells will not be acceptable. The ratio of $12D_{26}/h^2 A_{22}$ is the same as the dimensionless D_{16} if the complement of the lamination angle is used.

SECTION 8

ANGLE-PLY COMPOSITES – EXPERIMENTAL VERIFICATION

8.1 EXPERIMENTAL PROCEDURE

The experimental procedure used for the verification of the material coefficients of angle-ply composites paralleled closely that used for the cross-ply composites. Again, measurements of the A', B', and D' matrices were made instead of the A, B, and D matrices, because stress resultants N_i and bending moments M_i were the independent variables. Three-element strain rosettes were bonded to both sides of 0° and 90° beams. Uniaxial tensile loads and bending moments were applied to the beams sequentially. From the recorded surface strains, the in-plane strains and curvatures were computed in the same straightforward manner as before.

The total number of layers was limited to two and three. The n = 2 case was chosen because for this case the values of B_{16} and B_{26} were maximum; i. e., the strongest coupling existed between the in-plane strain and twisting moment or between the bending curvature and shear stress resultant. The n = 3 case was chosen because the values of A_{16}, A_{26}, D_{16}, and D_{26} were maximum; i. e., maximum deviations from orthotropic symmetry of the A and D matrices existed. The figures in the preceding section showed the above effects.

8.2 EXPERIMENTAL RESULTS

Measurements were made on angle-ply composites with various lamination angles. The theoretical predictions of the material coefficients were computed from the data in Equation (6. 1). In Figure 16, good agreement

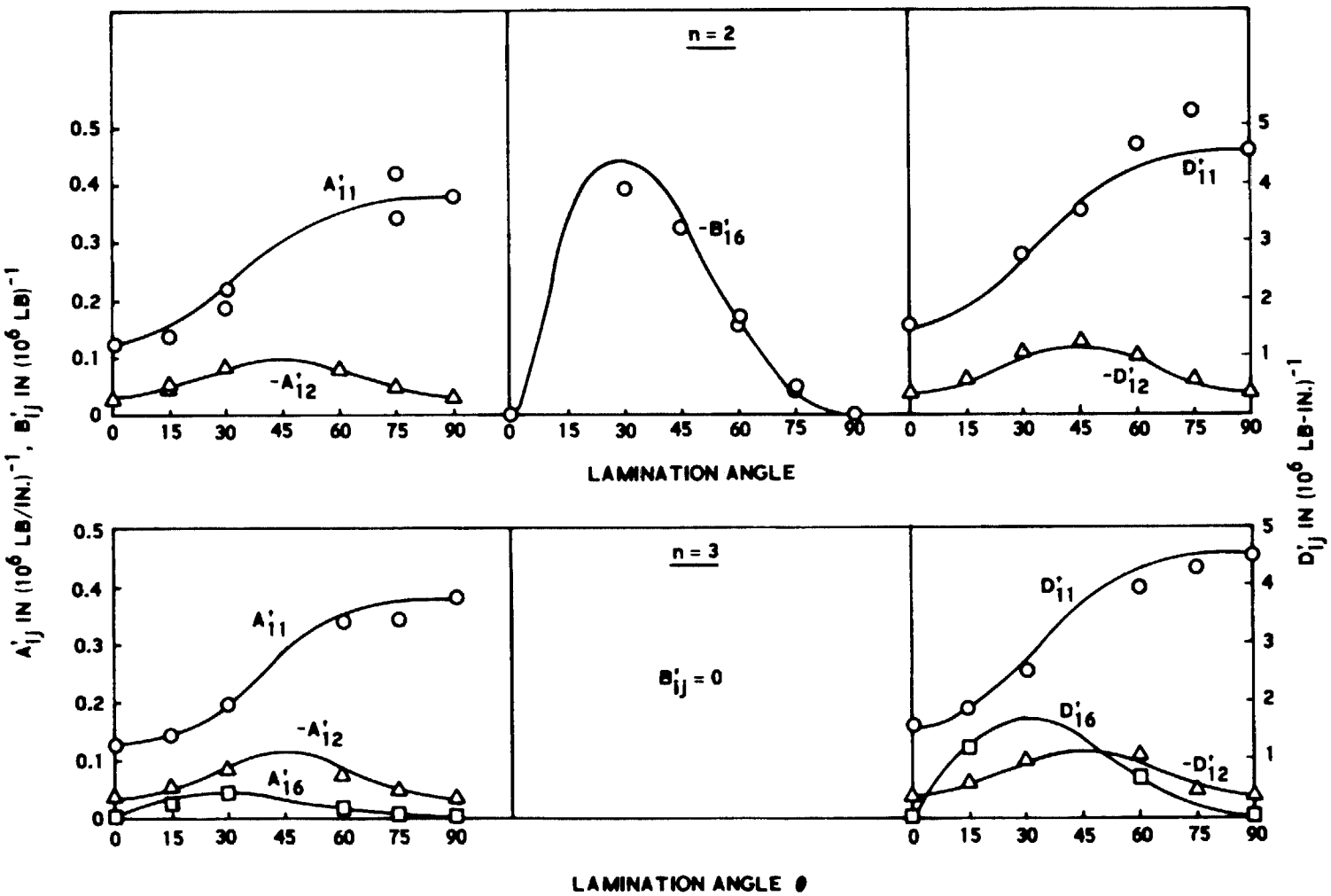

Figure 16. Angle-Ply Composites

between the theoretical and experimental results is shown. The unidirectional composite corresponds to the 0° and 90° cases.

The theoretical curves for A_{22}, A_{26}, B_{26}, D_{22}, and D_{26} were not shown. They were the mirror images (at 45°) of A_{11}, A_{16}, B_{16}, D_{11}, and D_{16}, respectively. Also omitted from Figure 15 were A_{66} and D_{66}.

8.3 CONCLUSIONS

For n = 2, a cross coupling caused by B_{16} and B_{26} exists. This is a source of internally induced shear stress in an angle-ply composite that is additive to the externally imposed stresses. This is similar to the coupling caused by B_{11} and B_{22} in the cross-ply composite, except that there the induced stresses are normal stresses.

For n = 3, it is seen that the types of elastic symmetry for the A and D matrices are changed from orthotropic symmetries at 0° and 90° to states of general anisotropy (i.e., no symmetry at all).

Based on the experimental results obtained here, the following can be concluded:

(1) The properties of unidirectional composites do transform in accordance with the fourth-rank tensor; thus, the use of the generalized Hooke's law is justified.

(2) The assumptions of the classical theory of anisotropic plates are reasonable.

(3) The original data for the unidirectional composite, as shown in Equation (6.1), are accurate; otherwise the variations of the A, B, and D matrices with the lamination angle would not agree with the measured data.

SECTION 9

LAMINATED PRESSURE VESSELS

9.1 THEORY OF LAMINATED PRESSURE VESSELS

For cylindrical pressure vessels of thin-wall construction, the membrane theory of shells is applicable. The stress resultants caused by internal pressure are

$$N_H = PR, \; N_L = PR/2 \tag{9.1}$$

where subscripts H and L denote hoop and longitudinal directions, respectively. Using the inverted constitutive Equation (4.10) for cross-ply cylinders,

$$\begin{bmatrix} \epsilon^o_H \\ \\ \epsilon^o_L \end{bmatrix} = \begin{bmatrix} A^*_{11} & A^*_{12} \\ \\ A^*_{12} & A^*_{22} \end{bmatrix} \begin{bmatrix} N_H \\ \\ N_L \end{bmatrix} \tag{9.2}$$

where direction 1 = hoop; direction 2 = longitudinal. Combining Equations (9.1) and (9.2),

$$\begin{aligned} \epsilon^o_H &= (A^*_{11} + A^*_{12}/2)\, PR \\ \\ \epsilon^o_L &= (A^*_{12} + A^*_{22}/2)\, PR \end{aligned} \tag{9.3}$$

It is more convenient to rearrange Equation (9.3) as follows:

$$\frac{E_{11}\, h}{PR}\ \epsilon_H^o = (A_{11}^* + A_{12}^*/2)\, E_{11}\, h$$

$$\frac{E_{11}\, h}{PR}\ \epsilon_L^o = (A_{12}^* + A_{22}^*/2)\, E_{11}\, h \qquad (9.4)$$

where E_{11} = axial stiffness of the unidirectional composite and h = total shell thickness.

Netting analysis, on the other hand, predicts the following relations:

$$\frac{E_{11}\, h}{PR}\ \epsilon_H^o = \frac{1+m}{m}$$

$$\frac{E_{11} h}{PR}\ \epsilon_L^o = \frac{1+m}{2} \qquad (9.5)$$

where m = cross-ply ratio = h_H/h_L.

The difference between the continuum analysis (9.4) and the netting analysis (9.5) is quite substantial. According to the former, the resultant strains are dependent on material coefficients A_{11}^*, A_{12}^*, and A_{22}^*. These coefficients are, in general, functions of all the original anisotropic constants of the unidirectional composite and the cross-ply ratio m. The netting analysis predicts that the strains are only functions of m.

9.2 EXPERIMENTAL RESULTS

Cylindrical pressure vessels with various values of cross-ply ratios were made and tested. The resultant surface strains are plotted in Figure 17, together with the theoretical predictions of both netting and continuum analyses. Unidirectional vessels (hoop winding only) correspond to $m = \infty$, but for these particular vessels m = 10 is reasonably close to $m = \infty$ so far as the strains are concerned.

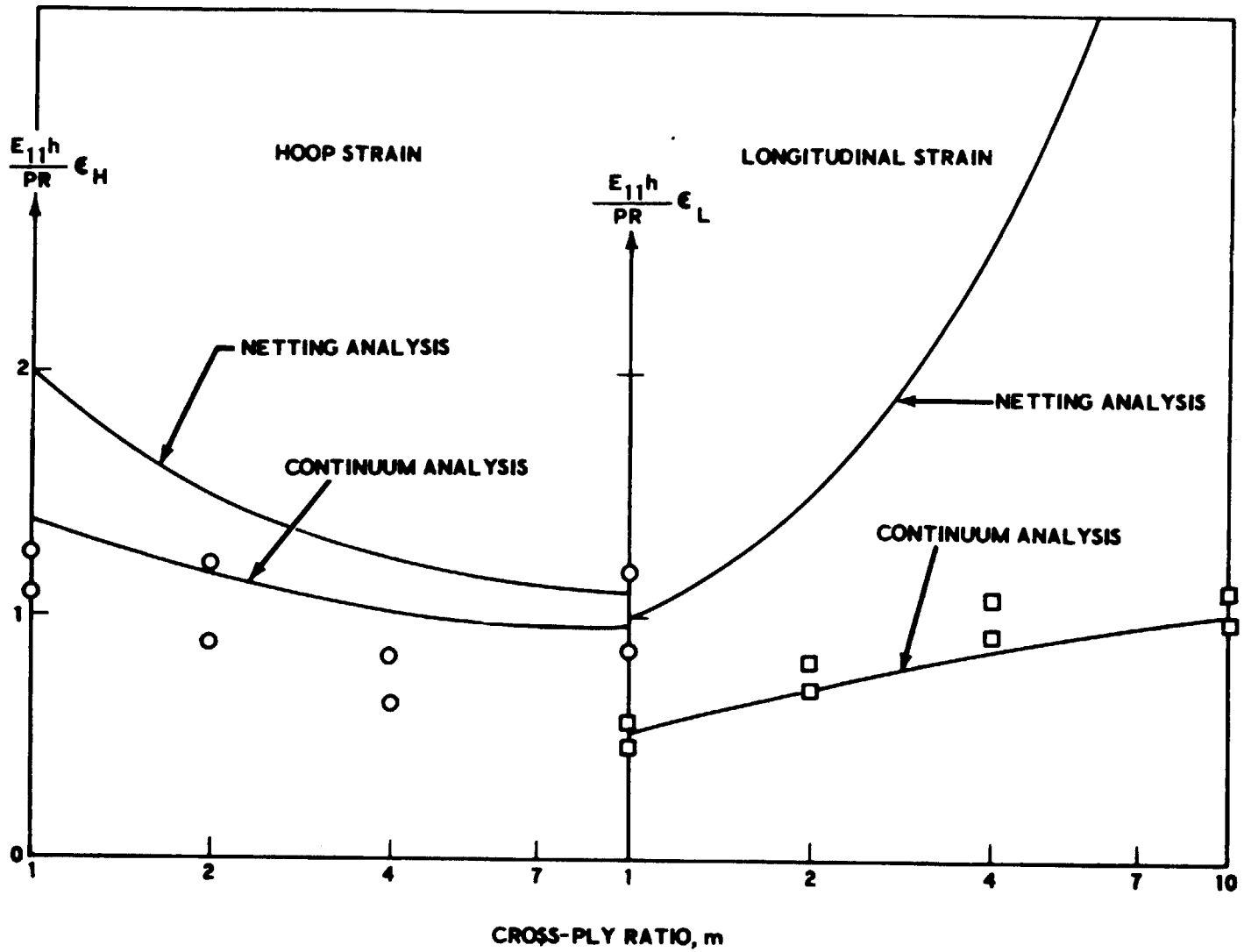

Figure 17. Cross-Ply Cylinder

From the experimental results, it is clear that the continuum analysis is more exact than netting analysis, particularly in the prediction of the longitudinal strain. The maximum level of strain was about 500 micro-inches per inch. The pressure-strain relations were linear and elastic.

9.3 CONCLUSIONS

The experimental confirmation of cross-ply laminated pressure vessels was adequate to establish the basis of continuum analysis. The significance of the continuum analysis extends beyond the determination of strains. The stress distribution, for example, can be computed from the constitutive equation of Section 4 in a straightforward manner. In a cylindrical pressure vessel, geometric constraint prohibits induced curvatures; i. e., cylindrical sections remain cylindrical.

From Equation (4. 12),

$$M = H^{*} N \tag{9.6}$$

where M = internally induced moments caused by zero curvature. The moments would, in turn, affect the complete stress distribution in the pressure vessel. In the prediction of strength, the induced stress and the initial stress must all be added to the externally imposed stress. The exact level of total stress must be known before one can assert what the "glass stress" or any other stress is.

SECTION 10

CONCLUSIONS

10.1 STATEMENT OF WORK ACCOMPLISHED

The work accomplished to date can be summarized as follows:

(1) Development of a theoretical basis for the prediction of the gross behavior of fiber-reinforced composites from the characteristics of the constituent materials. Included in the development are:

   (a) An evaluation of the relationship and contribution of the fiber and the matrix properties, matrix content, composite density, and the geometric configuration, as represented by Equation (2.2).

   (b) The constitutive equations governing the unidirectional composite, laminated composites (cross-ply and angle-ply), and pressure vessels, as shown in Equations (2.1), (4.3), and (9.2), respectively. The effects of lamination parameters on the material coefficients of the cross-ply and angle-ply composites are shown in Sections 5 and 7, respectively.

(2) Use of suitable experimental technique to verify the theoretical predictions of Item (1). Testing has been limited to include a minimum of experiments for verification. Existing data other than the axial stiffness of the unidirectional composite, E_{11}, have not been found.

10.2 LIMITATIONS OF THE THEORETICAL PREDICTIONS

The limitation of the theoretical predictions are summarized as follows:

a. Unidirectional Composites

(1) The unidirectional composite is quasi-homogeneous; i. e., the diameters of the fiber or filament must be small in comparison with the thickness of the unidirectional composite, and the filament distribution must be fairly uniform.

(2) The constituent materials, the filament and the matrix, are homogeneous, isotropic, and linearly elastic.

(3) A perfect mechanical bond exists between the filaments and the matrix.

(4) All filaments are parallel and continuous.

(5) The unidirectional composite is in the form of a thin plate or layer (i. e., a two-dimensional body).

(6) The unidirectional composite is a two-phase material; i. e., it contains no air bubbles or other foreign matter.

b. Laminated Composites

(1) The laminated composite consists of perfectly bonded layers of unidirectional composites of Item a.

(2) The total thickness of the laminated composite is small in comparison with the length and width of the composite. The displacement imposed on the composite is small, assuring the validity of this assumption that normals to the middle surface are nondeformable.

10.3 DEFINITION OF FUTURE PROBLEM AREAS

Future problem areas shall include the following as natural extensions of the present work:

(1) Elasticity analysis of stress concentrations caused by openings, vibration, buckling, thermal-elasticity, and so forth.

(2) Strength analysis, which will include the effects of initial stress (arising from curing), internally induced stress (arising from mechanical coupling, the B matrix), and structural breakdown of perfect bonding ("crazing").

(3) Recommendation of test methods for quality control and design data generation.

(4) Materials optimization for various structural configurations.

10.4 CONCLUDING STATEMENT

This study has shown the range of mechanical properties derivable from composite materials. By using glass filaments and epoxy resin as the basic constituents, unidirectional and laminated composites with vastly different properties can be made. Needless to say, other materials can be used as the constituents in order to produce an even wider range of useful mechanical properties. The material coefficients of the appropriate constitutive equation are expressed as analytical functions (as opposed to empirical functions) of various important geometric and material parameters of the composite. With the analytical functions, materials optimization in terms of stress, stiffness, or weight can be achieved in an exact fashion—by simple differentiations with no necessity for additional assumptions.

The present study has established a rational basis for the analysis of composite structures. Other multiphase composites can be similarly analyzed. Composites such as sandwich plates (C_{ij} = isotropic, n = 3), plywood (C_{ij} = orthotropic, n = 3, 5, 7) and others are special cases of the general laminated anisotropic composite covered in this study. The general laminated composite is inherently heterogeneous and anisotropic. This provides an enormous flexibility in designing the composite material to meet a specific structural requirement, e.g., the 2:1 ratio of the principal stresses of cylindrical pressure vessels. It is equally interesting that by selecting the proper lamination parameters a laminated anisotropic composite can be made to behave as a homogeneous and/or isotropic composite.[24] Thus, both the degrees of heterogeneity and anisotropy are controllable.

Netting analysis is not a reasonable theory for filament-wound materials. The continuum analysis outlined in this study is shown to be much more realistic, and, more importantly, the analysis can be extended to describe other types of structural behavior, e.g., the vibration and elastic stability of the composite. It is believed that filament-wound materials have not been utilized to their fullest potential. With added understanding of their behavior, it is hoped that a reliable basis of optimum design can be established in the near future.

REFERENCES

1. G. Slayter, "Two-phase Materials," Scientific American, January 1962, pp. 124-134.

2. P. M. Goodwin, "Constructing Composite Materials," Mechanical Engineering, December 1963, pp. 27-30.

3. B. Paul, "Prediction of Elastic Constants of Multi-phase Materials," Trans. AIME, Vol. 218, 1960, pp. 36-41.

4. Z. Hashin, "The Elastic Moduli of Heterogeneous Materials," J. App. Mech., Vol. 29, March 1962, pp. 143-150.

5. D. P. Hanley and R. F. H. Woodberry, "Highlights of Other ABL Sponsored Research Investigations," Proc. Fourth Semiannual Polaris Glass Reinforced Plastic R&D Conference, January 1963.

6. R. Hill, "Elastic Properties of Reinforced Solids: Some Theoretical Principles," J. Mech. Phys. Solids, Vol. 11, 1963, pp. 357-372.

7. Z. Hashin and S. Shtrikman, "On Effective Elastic Moduli of Multi-phase Materials and Polycrystals," Proc. of Fourth U.S. National Congress of Applied Mechanics, June 1962, pp. 619-625.

8. O. Hoffman, "Stresses and Deformations in Filament-Reinforced Structures," IAS paper No. 62-26, January 1962.

9. F. Beer, "Die Festigkeitseigenschaften Kreuzweise bewehrter Kunstoffe," VDI-Z, Vol. 101, April 1959, pp. 463-468.

10. J. T. Hofeditz, "Structural Design Considerations for Fiber Glass Pressure Vessels," Proc. 18th Annual Technical and Management Conference, Reinforced Plastic Division, Soc. Plastic Industry, February 1963, Sect. 7-C.

11. W. T. Walker, "Material Design Properties for Filament-Wound Construction," Proc. Fourth Semiannual Polaris Glass Reinforced Plastic R&D Conference, January 1963.

12. H. R. Jacobsen, "Optimum Construction of Reinforced Plastic Cylinders Subjected to High External Pressure," Douglas Missile and Space Systems Division, Report No. SM-44057, June 1963.

13. Z. Hashin and B. W. Rosen, "The Elastic Moduli of Fiber-Reinforced Materials," ASME Winter Annual Meeting, Paper 63-WA-175, November 1963.

REFERENCES (Continued)

14. L. R. Herrmann and K. S. Pister, "Composite Properties of Filament Resin Systems," ASME Winter Annual Meeting, Paper 63-WA-239, November 1963.

15. S. G. Lekhnitskiy, "Anisotropic Plates," 2nd Ed., Moscow, 1957.

16. S. W. Tsai, "A Variational Formulation of Two-Dimensional Heterogeneous Media," Aeronutronic Publication No. U-1698, June 1962.

17. S. W. Tsai, "Composite Stiffnesses of Fiber-Reinforced Media," Aeronutronic Publication No. U-1699, June 1962.

18. S. Timoshenko and J. N. Goodier, Theory of Elasticity, 2nd Ed., New York, 1951.

19. S. W. Tsai, G. S. Springer and A. B. Schultz, "The Composite Behavior of Filament-Wound Materials," Fourteenth International Astronautical Congress, Paris, France, September 1963, Paper No. 139.

20. H. L. Runyan and R. W. Leonard, "Research, Design Considerations, and Technological Problems of Structures for Launch Vehicles," Proc. NASA-University Conference on Science and Technology of Space Exploration, Vol. 2, November 1962, pp. 487-498.

21. R. R. Heldenfels and A. Hurlich, "Structures and Materials," Astronautics and Aerospace Engineering, November 1963, pp. 75-78.

22. E. Reissner and Y. Stavsky, "Bending and Stretching of Certain Types of Heterogeneous Aeolotropic Elastic Plates," J. Appl. Mech., Vol. 28, September 1961, pp. 402-408.

23. R. G. Dong and S. B. Dong, "Analysis of Slightly Anisotropic Shells," AIAA J., Vol. 1, 1963, pp. 2565-2569.

24. E. R. Scheyhing, "Structural Laminates With Composite Orthotropic/Isotropic Elastic Properties," Aeronutronic Publication No. U-2301, September 1963.